Solid State NMR and X-ray Diffraction Studies of Structure and Molecular Motion in *ansa*-Titanocenes

Alison J. Edwards,[†,‡] Nicholas J. Burke,[§] Christopher M. Dobson,[†,§] Keith Prout,*[,‡] and Stephen J. Heyes*[,§]

Contribution from the Inorganic Chemistry Laboratory, University of Oxford, South Parks Road, Oxford OX1 3QR, U.K., the Oxford Centre for Molecular Sciences, University of Oxford, South Parks Road, Oxford OX1 3QT, U.K., and the Chemical Crystallography Laboratory, University of Oxford, 9 Parks Road, Oxford OX1 3PD, U.K.

Received October 3, 1994[⊗]

Abstract: The structures and dynamics of a family of crystalline *ansa*-metallocenes, $[(C_5H_4)_2\text{-}C_2Me_4]TiX_2$ (X = F (**1**), Cl (**2**), Br (**3**), and I (**4**)), have been elucidated by the joint application of solid state NMR and single crystal X-ray diffraction techniques. X-ray crystal structures at ambient temperature indicate a single molecule with noncrystallographic 2-fold symmetry in the asymmetric unit of **1**. The structure of **2** comprises two distinct layers which are each formed from only one of the two crystallographically distinct molecules found in the asymmetric unit. These two molecules have the same conformation, but do not have C_2 point symmetry. The structure of **3** has four molecules per asymmetric unit; one has axial symmetry, but the others deviate from this to a greater extent than do the molecules of **2**. A layer structure with bromine atoms at the layer surfaces is discernible in **3**, but in contrast to **2** each layer contains all of the crystallographically distinct molecules. The structure of **4** has a single molecule in its asymmetric unit, of similar nonaxial conformation to those of **2**. The most noticeable feature is channels of iodine atoms parallel to the *c*-axis. The eight distinct molecules of these structures are placed into three conformational categories based on their deviation from axial symmetry. The surprisingly different structures for different halogens appear to be due to increasing halogen−halogen interaction, I > Br > Cl > F, in the preferred intermolecular contacts. ^{13}C CP/MAS NMR spectra in the temperature range 200−380 K show resonance multiplicities consistent with the crystallographically determined asymmetric units. Spectra for **2**, **3**, and **4** show significant changes with temperature, indicating the occurrence of activated exchange processes. 1D and 2D magnetization transfer experiments below 300 K and line shape simulations of exchange-broadening phenomena above 300 K indicate that for **4** and for one of the molecules in **2** a pairwise exchange process occurs. The other molecule in **2** remains rigid, indicating that packing interactions between the layers of the structure of **2** do not influence the barriers to the dynamic process. The measured Arrhenius activation barriers, E_a = 87 kJ mol^{-1} for **4** and 86 kJ mol^{-1} for the dynamic molecule of **2**, are remarkably similar given the dissimilarity of the molecular packing in crystals of **2** and **4**. All of the molecules of **3** show dynamic behavior; the resonances of one molecule are broadened even at 200 K, those for two of the others are in the coalescence regime at ca. 250 K, and the resonances of the fourth only broaden above 300 K. ^2H NMR quadrupole echo line shapes of a perdeuterated sample of **4** indicate only small changes between 296 and 480 K. The X-ray structures of all four compounds show no suggestion of disorder, the atomic displacement parameters are unremarkable, all the electron density is accounted for by the structure solutions, and there is no significant diffuse scatter in the X-ray photographs. The joint interpretation of the NMR and X-ray data indicates that the dynamic processes detected for **2**−**4** by NMR are not the expected enantiomeric exchange process, which is observed to be facile in solution. Both the NMR and X-ray data are, however, consistent with a hypothesis that a 180° reorientation about the pseudo-C_2 axis, bisecting the X−Ti−X interbond angle, occurs in the crystal concomitant with a small polytopal relaxation about the metal center. This process averages carbon atoms in a pairwise manner, but leads to no atomic positional disorder, and it averages the ^2H efg and ^{13}C CSA tensors only slightly. This motion constitutes an interesting dynamic mode of a molecular crystal, which is intermediate between the well-established examples of the effectively isotropic overall molecular reorientational disorder characteristic of a plastically crystalline phase and the disorder or fluxionality of specific groups or moieties within a molecule. Crystal data: (**1**) triclinic, $P\bar{1}$, a = 11.934(2), b = 8.5057(7), and c = 7.718(1) Å, α = 108.091(1), β = 110.71(1), and γ = 90.916(9)°, Z = 2, R = 0.033, R_w = 0.039 for 253 parameters and 2488 reflections $I > 3\sigma I$. (**2**) monoclinic, $P2_1/a$, a = 13.014(2), b = 18.129(2), and c = 14.547(1) Å, β = 116.416(8)°, Z = 8, R = 0.046, R_w = 0.061 for 344 parameters, and 4635 reflections $I > 3\sigma I$. (**3**) triclinic, $P\bar{1}$, a = 13.597(2), b = 14.406(2), and c = 20.101(2) Å, α = 124.97(1), β = 91.46(1), and γ = 93.37(1)°, Z = 8, R = 0.039, R_w = 0.042 for 687 parameters and 5141 reflections $I > 3\sigma I$. (**4**) rhombohedral (hexagonal axes), $R3c$, a = 24.608(7) and c = 14.741(1)Å, Z = 18, R = 0.032, R_w = 0.035 for 172 parameters and 765 reflections $I > 3\sigma I$.

Introduction

The *ansa*-metallocenes are bis(cyclopentadienyl) metal complexes in which the two cyclopentadienyl rings are bridged by one or more connecting atoms.[1] Chiral *ansa*-metallocene derivatives of the Group IV transition metals are of considerable interest as Ziegler−Natta catalysts for the stereospecific polymerization of α-alkenes.[2] The stereoselectivity of these polymerization catalysts has its origin in steric interactions

[†] Oxford Centre for Molecular Sciences.
[‡] Chemical Crystallography Laboratory.
[§] Inorganic Chemistry Laboratory.
[⊗] Abstract published in *Advance ACS Abstracts*, March 1, 1995.

(1) Smith, J. A.; von Seyerl, J.; Huttner, G.; Brintzinger, H.-H. *J. Organomet. Chem.* **1979**, *173*, 175−185.

0002-7863/95/1517-4637$09.00/0

between the growing substituted alkane chain and the chiral ligand framework.[3] For example, the stereoselectivity is found to increase if the *ansa* ligand has sterically demanding β substituents on both cyclopentadienyl rings.[4] Considerable interest has therefore been generated in the study of the conformations of these molecules in the solid state and in solution.[5] Numerous structures of Group IV chiral *ansa*-metallocenes have been determined. C_2 molecular symmetry is often observed for these *ansa*-metallocenes, but in many other structures the C_2 symmetry is removed since the *ansa* ligand is twisted out of axial alignment with the MX_2 group by up to 30° or more. That there is very little energy difference between these cases is evident from the observation of two crystal forms of *rac*-$[C_2H_4(C_5H_3\text{-}3\text{-}Bu^t)_2]TiCl_2$: one containing molecules of C_2 symmetry; the other with molecules twisted from axiality.[6] Also, the structure of $[(CH_3)_2Si(C_5H_4)_2]Zr(CH_2)_2Si(CH_3)_2$ contains two molecules in the asymmetric unit: one is axial; the other deviates by $\theta \approx 20°$.[7] Molecular mechanical calculations indicate that the intramolecular potentials are not very different in the range $\theta \approx \pm 30°$.[5] *Ansa*-metallocenes with conformations distorted from C_{2v} symmetry exist in two enantiomeric forms. However, even in such cases solution NMR spectra are consistent with planar symmetry. This indicates that the enantiomeric forms may interconvert in a facile manner through an eclipsed intermediate by a mechanism which involves the contrarotation of the two cyclopentadienyl rings. Typically this process is not frozen out even at 193 K.[5] Addition of bulky groups to the rings has enabled line broadening, but not decoalescence, to be observed in the 125 MHz ^{13}C NMR of $[(C_5H_3\text{-}3\text{-}Bu^t)C_2H_4(C_5H_3\text{-}4\text{-}Bu^t)]TiCl_2$ at 158 K.[8] Hindering the motion by introducing unfavorable contacts in the transition state to motion between naphthyl groups has enabled coalescence to be observed at 283 K and the slow limit of exchange to be reached at 213 K for [(*R*)-(−)-2,2′-bis(1-indenylmethyl)-1,1′-binaphthyl]titanium dichloride.[9] Finally, the crystal structure of 2,2′-ethylenebis(η^5-indenyl)$TiCl_2$ shows disorder over two enantiomeric forms, and it is postulated that the disorder may be of a dynamic nature.[10]

We were therefore interested in studying the structure and dynamics of *ansa*-metallocenes in the crystalline state. We have chosen to examine a related group of *ansa*-titanocene dihalides with a tetramethylethylene bridge.[4] We present here a systematic investigation of the *ansa*-metallocene complexes of general formula $[(C_5H_4)C(CH_3)_2C(CH_3)_2(C_5H_4)]TiX_2$ (X = F (**1**), Cl (**2**), Br (**3**), or I (**4**)) using a combination of single-crystal X-ray diffraction and solid state ^{13}C CP/MAS and ^2H NMR techniques.

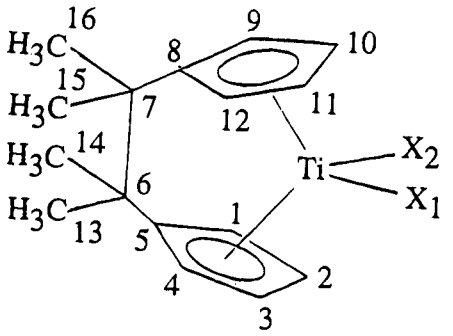

Figure 1. Schematic diagram of the tetramethylethylene-bridged *ansa*-titanocenes, showing the atomic numbering scheme used.

A schematic structure of the *ansa*-titanocenes **1**−**4**, illustrating the atom numbering system used throughout, is shown in Figure 1.

Experimental Section

(i) **Preparation and Characterization.** All solutions were handled on a dual vacuum/nitrogen line using standard Schlenk techniques. All solvents were predried over molecular sieves and, in addition, petroleum ether (bp 40−60 °C) was distilled from a sodium/potassium alloy, tetrahydrofuran from potassium metal, and dichloromethane from CaH_2. The dry, solid *ansa*-metallocenes were handled in air when necessary but were stored under a dry nitrogen atmosphere.

6,6-Dimethylfulvene, prepared by the method of Stone and Little,[11] was coupled through a Grignard reduction, and the various tetramethylethylene-bridged titanocene compounds were prepared by reaction with the appropriate TiX_4 using the method of Schwemlein and Brintzinger.[12] All samples were characterized by ^1H and ^{13}C NMR spectroscopy in $CDCl_3$ solution (at 300.13 and 75.5 MHz, respectively, on a Bruker AM300 spectrometer) and by elemental analysis (C/H, Ti, and halogen). Pure materials were recrystallized subsequently by a variety of crystallization techniques in order to obtain samples for solid state NMR spectroscopy and X-ray diffraction experiments. Methods used included slow cooling to 193 K of solutions in CH_2Cl_2 or petroleum ether (bp 40−60 °C) or of mixtures created by dissolution in CH_2Cl_2 followed by layering with petroleum ether (bp 40−60 °C) and slow diffusional mixing. Slow evaporation through a pinhole, at ambient temperature, of solutions in CH_2Cl_2, petroleum ether (bp 40−60 °C), acetone, or mixtures of CH_2Cl_2 and petroleum ether (bp 40−60 °C) was also used. In some cases there was evidence for mixtures of polymorphs, and the recrystallization technique used in each case is documented in the figure legends.

For preparation of deuterated samples, dimethylfulvene was deuterated prior to the coupling reaction by a modification of the OD^- exchange method of Lambert and Finzel,[13] reported originally for the deuteration of cyclopentadiene. Three exchanges resulted in dimethylfulvene (D = 95+%) (by mass spectrometric analysis using an AEI MSS 902 machine). It was found to be particularly important to dry the exchanged dimethylfulvene-d_{10} with anhydrous $MgSO_4$ before the Grignard coupling reaction. Exchange of the deuterium did not occur in the further steps of the synthesis, as evidenced by monitoring with ^1H and ^2H NMR spectroscopy. The purified deuterated tetramethylethylene titanocene diiodide was characterized by ^2H NMR (46.05 MHz) in $CHCl_3$ solution using a Bruker AM300 spectrometer.

(ii) **Solid State NMR Spectroscopy.** ^{13}C CP/MAS NMR spectra were acquired on a Bruker MSL 200 spectrometer equipped with an Oxford Instruments 4.7 T wide-bore (98 mm) superconducting solenoid magnet operating at frequencies of 50.32 and 200.13 MHz for ^{13}C and ^1H, respectively. Acquisition and processing of data were controlled by an Aspect 3000 computer. CP/MAS spectra were recorded using a multinuclear, proton-enhanced, double-bearing magic angle sample spinning probe (Bruker Z32-DR-MAS-7DB), utilizing dry nitrogen for

(2) Brintzinger, H.-H. In *Transition Metals and Organometallics as Catalysts for Olefin Polymerization*; Kaminsky, W., Sinn, H., Eds.; Springer-Verlag: Berlin, 1988; pp 249−256. Röll, W.; Brintzinger, H.-H.; Rieger, B.; Zolk, R. *Angew. Chem., Int. Ed. Engl.* **1990**, *29*, 279−280. Jordan, R. F.; Bradley, P. K.; LaPointe, R. E.; Taylor, D. F. *New J. Chem.* **1990**, *14*, 505.

(3) Burger, P.; Hortmann, K.; Brintzinger, H.-H. *Makromol. Chem., Macromol. Symp.* **1993**, *66*, 127−140.

(4) Gutmann, S.; Burger, P.; Hund, H.-U.; Hofmann, J.; Brintzinger, H.-H. *J. Organomet. Chem.* **1989**, *369*, 343-357.

(5) Burger, P.; Diebold, J.; Gutmann, S.; Hund, H.-U.; Brintzinger, H.-H. *Organometallics* **1992**, *11*, 1319−1327.

(6) Collins, S.; Hong, Y.; Taylor, N. J. *Organometallics* **1990**, *9*, 2695−2703.

(7) Kabi-Satapathy, A.; Bajgur, C. S.; Reddy, K. P.; Petersen, J. L. *J. Organomet. Chem.* **1989**, *364*, 105−117.

(8) Collins, S.; Hong, Y.; Ramachandran, R.; Taylor, N. J. *Organometallics* **1991**, *10*, 2349−2356.

(9) Burk, M. J.; Colletti, S. L.; Halterman, R. L. *Organometallics* **1991**, *10*, 2998−3000.

(10) Parkin, S.; Hitchcock, S. R.; Hope, H.; Nantz, M. H. *Acta Crystallogr.* **1994**, *C50*, 169−171.

(11) Stone, K. J.; Little, R. D. *J. Org. Chem.* **1984**, *49*, 1849−1853.

(12) Schwemlein, H.; Brintzinger, H.-H. *J. Organomet. Chem.* **1983**, *254*, 69−73.

(13) Lambert, J. B.; Finzel, R. B. *J. Am. Chem. Soc.* **1983**, *105*, 1954−1958.

all gas requirements. Approximately 100−300 mg of sample was packed into 7 mm zirconia rotors with Kel-F or BN caps for MAS at typical rates of 1−5 kHz. A single contact spin-lock cross polarization (CP) sequence[14] was used with alternate cycle spin-temperature inversion[15] and flip-back of ^{1}H magnetization.[16] The ^{1}H rf field strength was 1.7 mT ($\omega_1 \approx 72$ kHz) and resulted in a 90° pulse length of 3.5 μs. Temperature measurement and regulation, utilizing a Bruker B-VT1000 unit equipped with a copper−constantan thermocouple and digital reference, was of the bearing gas. Temperature calibration was achieved both with the samarium ethanoate tetrahydrate Curie law ^{13}C NMR chemical shift thermometer,[17] previously set against the phase transitions of *d*-camphor,[17] cobaltocenium hexafluorophosphate,[18] and 1,4-diazabicyclo[2.2.2]octane,[17] and with the samarium stannate, $Sm_2Sn_2O_7$, Curie law ^{119}Sn NMR chemical shift thermometer.[19] Spectra were generally recorded with 3−5 K temperature increments and ca. 20 min was allowed for equilibration at each new temperature before commencement of spectral acquisition. Free induction decays were defined by ca. 2K data points over a spectral width of 20 kHz and were zero-filled to 16K data points prior to Fourier transformation. Typically 100−1500 transients, with a contact time of 1.5 ms and a relaxation delay of 3.5 s, were accumulated for each spectrum. Chemical shifts are reported on the δ scale with respect to δ(TMS) = 0 ppm and were referenced externally to the upfield resonance of solid adamantane at 29.5 ppm.[20] The ^{79}Br NMR spectrum of a small quantity of KBr included with the adamantane sample was used to calibrate accurately the magic angle.[21] Dipolar dephasing experiments,[22] using delays of 20−200 μs, were carried out using the pulse sequence of Alemany *et al.*[23] in which 180° pulses are applied simultaneously to the ^{1}H and ^{13}C spins half way through the delay time in order to refocus the effects of chemical shifts and other static field inhomogeneities. For T_1 determinations using CP/MAS NMR, Harbison *et al.*'s[24] modification of Torchia's experiment[25] was used, for which $M_{net} = (M_1 - M_2) = 2M_{CP}\exp(-t/T_1)$. Rotationally asynchronous TPPI phase-sensitive CP/MAS 2D-exchange NMR experiments with mixing times in the range 0.5−2 s were performed as described by Twyman and Dobson.[26] Typically, 512 increments of 62 μs in t_1 were recorded and the resulting data set was transformed in two dimensions to give 4K by 4K datapoints, usually with shifted sine bell apodization in both dimensions. 1D magnetization transfer measurements used the rotationally-synchronized, selective experiment of Conner *et al.*,[27] which monitors longitudinal polarization transfer between two selected resonances, and is effectively a single slice through the 2D exchange spectrum. Mutual exchange between two resonances was always checked by performing the exchange experiment in the reverse direction, and in cases where more that two peaks are involved in exchange the experiment was always performed for at least two pairs of resonances. Kinetic data were obtained from these magnetization transfer results following the analysis of Jeener *et al.*[28] for spin exchange between two sites of equal population, in which the ratio of intensities of the resonances after a mixing time, τ, is given by $M_B/M_A = r = [1 - \exp(-k\tau)]/[1 + \exp(-k\tau)]$ such that a plot of $\ln[(1 + r)/(1 - r)]$ versus τ yields, k, the modified rate of magnetization transfer, as the slope. For the ^{13}C NMR experiments performed here, spin diffusion can be neglected[29] and the rate of chemical exchange is obtained directly from the rate of magnetization transfer. The exchange-broadened line shapes of the ^{13}C CP/MAS NMR spectra at temperatures above ambient were simulated using the program DNMR4 (QCPE no. 466).[30] This program calculates the line shapes using a full density matrix approach[31] from two sets of input parameters, those from the static or slow limit spectrum and those describing the dynamic event, and relaxation and exchange rates. Rate data from both magnetization transfer experiments and exchange broadening simulations were used to determine Arrhenius activation parameters.

^{2}H NMR spectra were recorded on a Bruker MSL400 spectrometer at 61.42 MHz, using a Bruker HPWB73A high-power probe with a 7 mm horizontal solenoid coil. A 200 mg sample was packed into a glass tube and sealed *in vacuo*. The quadrupolar spin echo technique[32] with standard precautions[33] and phase cycling to remove off-resonance effects[34] was employed. All spectra were recorded using quadrature detection. Typically 2.5 μs 90° pulses and spin echo delay times of τ = 20−200 μs were employed. A recycle delay of 15 s was used throughout the temperature range. In the range 290−500 K, temperatures were accurate to ±1 K and stable to ±0.1 K. Between 30 min and 1 h was allowed for thermal equilibrium to be reached at each new temperature before spectral accumulation was commenced. Averaged ^{2}H NMR spectral line shapes in the fast limit of motional averaging were calculated[35] from order parameter theory,[36,37] assuming averaging by discrete jump processes between distinct molecular orientations. Spectral line shapes for the general case of spin exchange by a jump-type mechanism between discrete sites were calculated explicitly from modified Bloch expressions for the quadrupolar spin echo experiment.[37,38] Fuller details of the NMR line shape analysis are to be found elsewhere.[39]

(iii) **Single-Crystal X-ray Diffraction.** Crystals used for the X-ray structure analyses were obtained either by slow evaporation of solutions in dichloromethane/petroleum ether (bp 40−60 °C) (fluoride, bromide, and iodide) or by slow evaporation from acetone (chloride). The well-formed red crystals of the chloride and bromide compounds (**2** and **3**) diffracted strongly as did the small yellow crystal fragment of the fluoride compound (**1**), but the diffraction pattern obtained from the small crystal of the iodide compound (**4**) was of much lower intensity. Relevant details of the data collection are given in Table 1. Data reduction included Lorentz and polarization corrections. All four structures were solved by direct methods using SHELXS-86[40] which yielded all non-hydrogen atom positions for the fluoride (**1**) and chloride (**2**) structures and all heavy atom positions and some carbon atom positions for the bromide (**3**) and iodide (**4**). For the bromide (**3**) and iodide (**4**), the partial model from direct methods was developed by Fourier refinement until all atoms except hydrogen were located.

(14) Pines, A.; Gibby, M. G.; Waugh, J. S. *J. Chem. Phys.* **1973**, *59*, 569−590. Yannoni, C. S. *Acc. Chem. Res.* **1982**, *15*, 201−208.
(15) Stejskal, E. O.; Schaefer, J. *J. Magn. Reson.* **1975**, *18*, 560−563.
(16) Tegenfeldt, J.; Haeberlen, U. *J. Magn. Reson.* **1979**, *36*, 453−457.
(17) Haw, J. F.; Campbell, G. C.; Crosby, R. C. *Anal. Chem.* **1986**, *58*, 3172−3177.
(18) Heyes, S. J. D. Ph.D. Thesis, University of Oxford, 1989.
(19) Grey, C. P.; Cheetham, A. K.; Dobson, C. M. *J. Magn. Reson.* **1993**, *A101*, 299−306.
(20) Earl, W. L.; VanderHart, D. L. *J. Magn. Reson.* **1982**, *48*, 35−54.
(21) Frye, J. S.; Maciel, G. E. *J. Magn. Reson.* **1982**, *48*, 125−131.
(22) Opella, S. J.; Frey, M. H. *J. Am. Chem. Soc.* **1979**, *101*, 5854−5856.
(23) Alemany, L. B.; Grant, D. M.; Alger, T. D.; Pugmire, R. J. *J. Am. Chem. Soc.* **1983**, *105*, 6697−6704.
(24) Harbison, G. S.; Smith, S. O.; Pardoen, J. A.; Courtin, J. M. L.; Lugtenburg, J.; Herzfeld, J.; Mathies, R. A.; Griffin, R. G. *Biochemistry* **1985**, *24*, 6955−6962.
(25) Torchia, D. A. *J. Magn. Reson.* **1978**, *30*, 613−616.
(26) Twyman, J. M.; Dobson, C. M. *Magn. Reson. Chem.* **1990**, *28*, 163−170.
(27) Conner, C.; Naito, A.; Takegoshi, K.; McDowell, C. A. *Chem. Phys. Lett.* **1985**, *113*, 123−128. Takegoshi, K.; McDowell, C. A. *J. Am. Chem. Soc.* **1986**, *108*, 6852−6857.
(28) Jeener, J.; Meier, B. H.; Bachmann, P.; Ernst, R. R. *J. Chem. Phys.* **1979**, *71*, 4546−4553.
(29) VanderHart, D. L. *J. Magn. Reson.* **1987**, *72*, 13−47.
(30) Bushweiler, C. H.; Letendre, L. J.; Brunelle, J. A.; Bilotsky, H. S.; Whalon, M. R.; Fleischmann, S. H. Quantum Chemistry Program Exchange Programme, Program No. 466, DNMR4.
(31) Binsch, G. *Mol. Phys.* **1968**, *15*, 469−478. Binsch, G. *J. Am. Chem. Soc.* **1969**, *91*, 1304−1309.
(32) Davis, J. H.; Jeffrey, K. R.; Bloom, M.; Valic, M. I.; Higgs, T. P. *Chem. Phys. Lett.* **1976**, *42*, 390−394.
(33) Ronemus, A. D.; Vold, R. L.; Vold, R. R. *J. Magn. Reson.* **1986**, *70*, 416−426. Hentschel, R.; Spiess, H. W. *J. Magn. Reson.* **1979**, *35*, 157−162.
(34) Bloom, M.; Davis, J. H.; Valic, M. I. *Can. J. Phys.* **1980**, *58*, 1510−1517.
(35) All computer programs for NMR simulations were written in FORTRAN and run on the Oxford University Computing Service's VAX CLUSTER system.
(36) Seelig, J. *Q. Rev. Biophys.* **1977**, *10*, 353−418.
(37) Wittebort, R. J.; Olejniczak, E. T.; Griffin, R. G. *J. Chem. Phys.* **1987**, *86*, 5411−5420.
(38) Greenfield, M. S.; Ronemus, A. D.; Vold, R. L.; Vold, R. R.; Ellis, P. D.; Raidy, T. E. *J. Magn. Reson.* **1987**, *72*, 89−107.
(39) Heyes, S. J.; Clayden, N. J.; Dobson, C. M. *J. Phys. Chem.* **1991**, *95*, 1547−1554.
(40) Sheldrick, G. M. In *Crystallographic Computing 3*; Sheldrick, G. M., Kruger, C., Goddard, R., Eds.; Oxford University Press: Oxford, 1985; pp 175−189.

Table 1. Crystal Data and Experimental Parameters for the X-ray Structure Analyses

formula	$C_{16}H_{20}TiF_2$	$C_{16}H_{20}TiCl_2$	$C_{16}H_{20}TiBr_2$	$C_{16}H_{20}TiI_2$
M_r	298.23	331.14	420.04	514.04
crystal system	triclinic	monoclinic	triclinic	rhombohedral
space group	$P\bar{1}$	$P2_{1/a}$	$P\bar{1}$	R3c
a (Å)	11.934(2)	13.014(1)	13.597(2)	24.608(7)
b (Å)	8.5057(7)	18.129(2)	14.406(2)	24.608(7)
c (Å)	7.718(1)	14.547(1)	20.101(2)	14.741(1)
α (deg)	108.091(9)	90	124.97(1)	90
β (deg)	110.71(1)	116.42(1)	91.46(1)	90
γ (deg)	90.916(9)	90	93.37(1)	120
cell vol. (Å^3)	689.6	3074	3212	7731
Z	2	8	8	18
D_c (g cm^{-3})	1.436	1.431	1.737	1.988
$F(000)$	312	1376	1664	4392
instrument	CAD4	CAD4	CAD4	CAD4
radiation	Cu Kα	Cu Kα	Cu Kα	Cu Kα
scan mode	$\omega-2\theta$	$\omega-2\theta$	$\omega-2\theta$	$\omega-2\theta$
θ range for data colln	$0 < 2\theta \leq 150°$	$0 < 2\theta \leq 150°$	$0 < 2\theta \leq 108°$	$0 < 2\theta \leq 110°$
scan angle	$0.90 + 0.15 \tan\theta$	$0.90 + 0.15 \tan\theta$	$0.65 + 0.15 \tan\theta$	$0.90 + 0.15 \tan\theta$
min, max h; k; l	−1,14; −10,10; −9,9	−1,16; −1,22; −18,18	−1,14; −14,15; −19,21	−1,26; −26,26; −1,15
no. reflns collected	3133	7865	7784	5931
no. unique reflns	2721	6296	6532	1245
R merge	0.020	0.054	0.024	0.074
no. observed $I \geq 3\sigma I$	2488	4635	5141	765
temperature (K)	293 ± 2	293 ± 2	293 ± 2	293 ± 2
crystal dim (mm)	0.3 × 0.4 × 0.8	0.6 × 0.6 × 0.8	0.3 × 0.3 × 0.5	0.1 × 0.1 × 0.3
μ (cm^{-1})	53.55	78.9	282.2	326.9
min, max, abs correction	0.824,1.321	0.430, 1.420	0.711, 1.331	0.595, 1.885
residual electron density (e Å^{-3})	min −0.34; max 0.39	min −0.47; max 0.49	min −0.5; max 0.7	min −0.5; max 0.5
final R, R_w	0.033, 0.039	0.046, 0.061	0.039, 0.042	0.032, 0.035

Positional and anisotropic displacement parameters for the non-hydrogen atoms were refined to convergence by the least squares method, minimizing $\sum w(F_{obs} - F_{calc})^2$ for all observed reflections. The full normal matrix was used for the fluoride (**1**), chloride (**2**), and iodide (**4**) and a large block approximation to the full matrix for the bromide (**3**). A Chebychev polynomial weighting scheme[41] was employed. For all four structures an empirical absorption correction (DIFABS[42]) was applied prior to final refinement. Hydrogen atoms were included in the models at geometrically idealized positions except for the fluoride (**1**) structure in which all hydrogen atoms were clearly evident and the relatively large number of observed reflections permitted their inclusion in the positional refinement with isotropic temperature parameters. Final residuals are given in Table 1. Except where indicated to the contrary, the Oxford CRYSTALS[43] system was used for all crystallographic calculations. Scattering factors were taken from International Tables.[44]

For the fluoride (**1**), all the observed lines in the sharp and extensive high-resolution X-ray powder diffractogram (measured on a Siemens D5000 powder diffractometer, Cu Kα radiation) of a sample of the bulk material used in the NMR experiments could be accounted for by the observed unit cell dimensions of the single crystal specimen, indicating that the bulk material was most probably a single polymorphic form. All the other bulk samples were checked by X-ray powder diffraction on a Philips PW1710 powder diffractometer and were shown using LAZY PULVERIX[45] to be monophasic and consistent with the single crystal data.

Results

(a) Solid State NMR Spectroscopy. (i) ^{13}C CP/MAS NMR Spectroscopy. ^{13}C CP/MAS NMR spectra were recorded for **1**−**4** over a temperature range of 200−380 K. Figure 2 shows for each compound the spectra at three temperatures chosen to illustrate the significant variations with temperature. The regions of the spectrum in which chemically similar carbons resonate are indicated. Assignments were made by comparison with those made in solution ^{13}C NMR spectra[46] and from dipolar dephasing experiments to identify the resonances of non-protonated carbons and methyl groups.

The spectrum of the iodide complex **4** at 299 K (Figure 2d) shows 16 isotropic resonances, as many peaks as there are carbon atoms in the molecule, consistent with a single molecule in the crystallographic asymmetric unit. As the temperature is raised above ambient, the spectra show clear evidence of the onset of exchange broadening and coalescence phenomena,[47] demonstrating that a dynamic process is occurring at a rate increasing progressively with temperature. By 350 K this process is approaching a rate at the fast limit of the exchange broadening time scale (10^3 s^{-1}). However, the spectrum, instead of sharpening into the fast limit, is subject to a further broadening, which increases in severity up to the maximum temperature studied (370 K). The broadening mechanisms are a result of the exchange process reaching a rate comparable firstly with the MAS rate[48] (3 kHz) and subsequently with the frequency of the high-power proton decoupling field[49] (70 kHz) used in the CP/MAS experiment. Due to the small residual CSA of the resonances of **4**, as indicated by the low intensity of the spinning sidebands, it is assumed that the dipolar broadening mechanism is dominant. Support is lent to this mechanism by the concurrent decrease in the effectiveness of CP, which results in poor signal-to-noise for the spectra at $T >$ 360 K. The maximum broadening regime is not reached by 380 K, and no kinetic data could be extracted from this mechanism.

(41) Carruthers, J. R.; Watkin, D. J. *Acta Crystallogr.* **1979**, *A35*, 698−699.
(42) Walker, N.; Stuart, D. *Acta Crystallogr.* **1983**, *A39*, 158−166.
(43) Watkin, D. J.; Carruthers, J. R.; Betteridge, P. W. *CRYSTALS User Guide*; Chemical Crystallography Laboratory: Oxford, 1985.
(44) Cromer, D. T.; Weber, J. T. *International Tables for X-ray Crystallography*; Ibers, J. A., Hamilton, W. C., Eds.; Kynoch Press: Birmingham, 1974; Vol. 4.
(45) Yvon, K.; Jeitschko, W.; Parthé, E. *LAZY PULVERIX*, Geneva, 1977.
(46) Gutmann, S.; Burger, P.; Prosenc, M.-H.; Brintzinger, H.-H. *J. Organomet. Chem.* **1990**, *397*, 21−28.
(47) Sandström, J. *Dynamic NMR Spectroscopy*; Academic Press: London, 1982.
(48) Suwelack, D.; Rothwell, W. P.; Waugh, J. S. *J. Chem. Phys.* **1980**, *73*, 2559−2569.
(49) Rothwell, W. P.; Waugh, J. S. *J. Chem. Phys.* **1981**, *74*, 2721−2732.

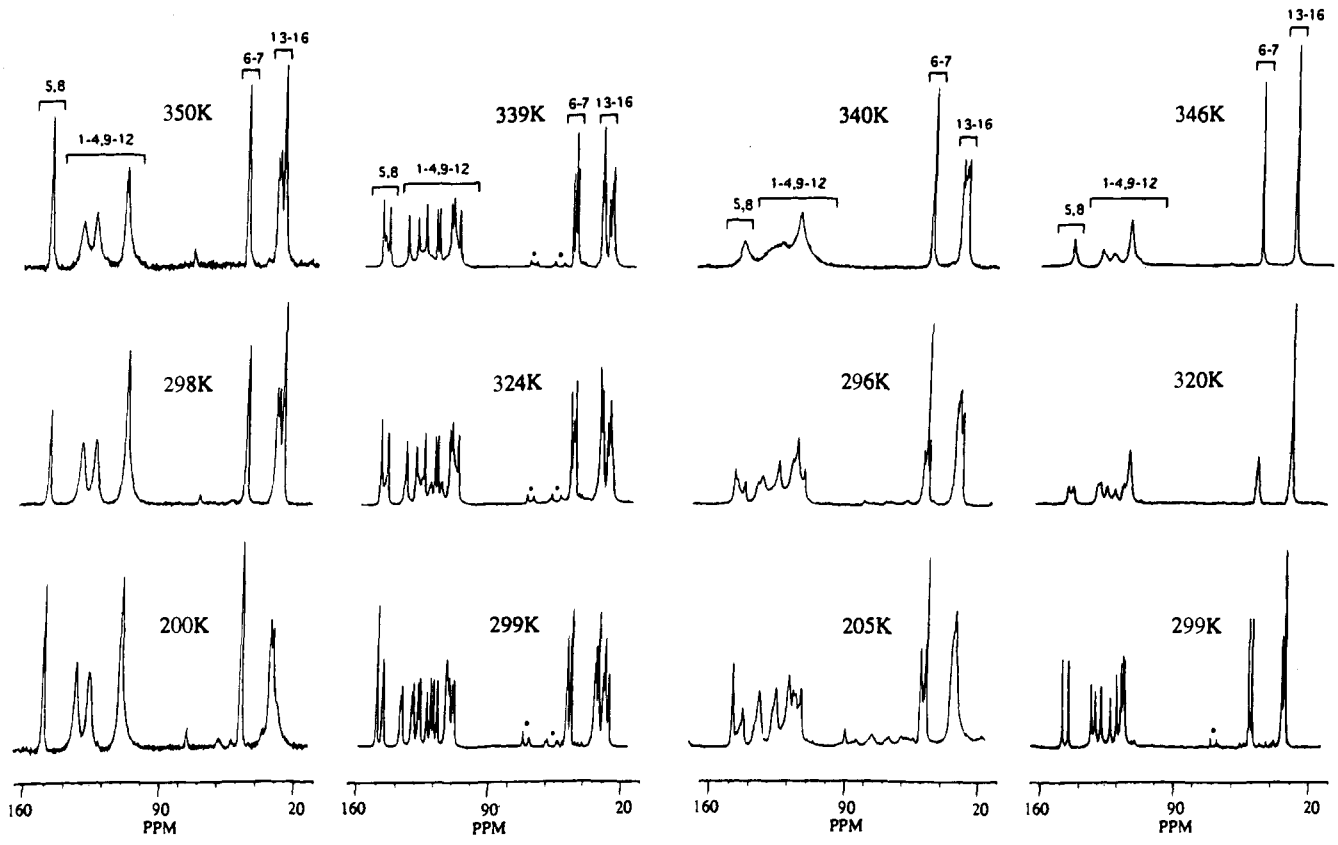

Figure 2. Representative ^{13}C CP/MAS NMR spectra of the *ansa*-titanocenes $[(C_5H_4)_2C_2Me_4]TiX_2$: (a) X = F (**1**) at 200, 298, and 350K, (b) X = Cl (**2**) at 299, 324, and 339 K, (c) X = Br (**3**) at 205, 296, and 340 K, and (d) X = I (**4**) at 299, 320, and 346 K.

The ^{13}C CP/MAS 2D exchange (magnetization transfer) NMR spectrum of **4** was recorded at 299 K using a mixing time of 0.7 s. The methyl carbon resonances undergo effective longitudinal relaxation within the mixing time and are not observed in this spectrum. Figure 3d presents a contour plot of the regions of the spectrum containing the cyclopentadienyl and bridge carbon atom resonances. The off-diagonal cross peaks observed delineate the exchange pathway of the dynamic process observed previously from the line broadening effects at higher temperatures. Examination of the contour plot shows that each peak undergoes an exclusive pairwise exchange with just one other peak in the spectrum, at a rate which is slow on the NMR time scale ($<10\ s^{-1}$). The peaks that are interconnected by the exchange process are of the same chemical type. These observations are consistent with the molecules undergoing an activated exchange process, which results in time-averaged 2-fold symmetry of the molecule.

The rate of exchange between the two resonances attributable to the *ipso* cyclopentadienyl carbons 5 and 8 was investigated in greater detail at five temperatures in the range 265−299 K using the selective 1D magnetization transfer experiment[27] at a range of mixing times at each temperature. At 299 K the experiment was repeated between the resonances at 121.4 and 126.3 ppm to prove that the exchange between all sites linked by cross peaks reflects the same molecular process. The derived values of the modified two-site exchange rate are collected in Table 2. Using the site permutations indicated by the 2D exchange spectrum, the spectra above ambient were simulated for the effects of exchange broadening. Experimental and simulated spectra for the *ipso* carbons 5 and 8 in the temperature range 265−339 K are shown in Figure 4a and the exchange rates are also recorded in Table 2. The rate data from both regimes show Arrhenius behavior, $k = A\exp(-E_a/RT)$ with $E_a = 87$ kJ mol^{-1} and $A = 4 \times 10^{16}$ s^{-1}. The consistency of the magnetization transfer and exchange broadening rate data indicates that it is the same activated process being observed throughout the temperature regime.

The ^{13}C CP/MAS NMR spectrum of the chloride complex (**2**) (as obtained by recrystallization from acetone)[50] at 299 K (Figure 2b) in contrast with that of the iodide **4** shows twice as many peaks as there are carbon atoms in the molecule. This suggests that for this compound there are two molecules in the crystallographic asymmetric unit.

The spectra above 300 K show the effects of exchange broadening and coalescence phenomena but are more complicated than those of **4**. Close examination of the high temperature spectra indicates that half of the resonances broaden in a manner that indicates exchange but that the others remain

(50) The method of recrystallization of **2** proved an important issue due to the occurrence of polymorphism. Samples recrystallized either from petroleum ether (bp 40−60 °C) or from acetone gave identical ^{13}C CP/MAS NMR spectra and X-ray powder diffractograms. X-ray powder diffractograms of material obtained from recrystallization in trichloromethane, either by evaporation or by layering with petroleum ether, indicated reflections identical to those observed in other samples, but also a large number of other reflections attributed to a different crystalline form of **2**. The ^{13}C CP/MAS NMR spectra of such samples were complex and included a resonance at 82.8 ppm, attributed to $CHCl_3$. On heating, this resonance diminished in intensity between 324 and 339 K, ultimately disappearing. In addition, there were simultaneously significant changes in other regions of the spectrum apparently related to the loss of $CHCl_3$. The spectral changes are irreversible, and the spectrum obtained on return to ambient temperature is identical to that of the acetone-recrystallized sample. The evidence suggests pseudopolymorphism, in which part of the sample exists as the $CHCl_3$ solvate. Irreversible solvent loss on heating causes reversion to the normal solvent-free crystalline phase. A single crystal recovered from acetone was powdered, and its ^{13}C CP/MAS NMR was recorded and found to be identical to that of the bulk material. All the spectra reported here are those of the phase obtained by recrystallization from acetone.

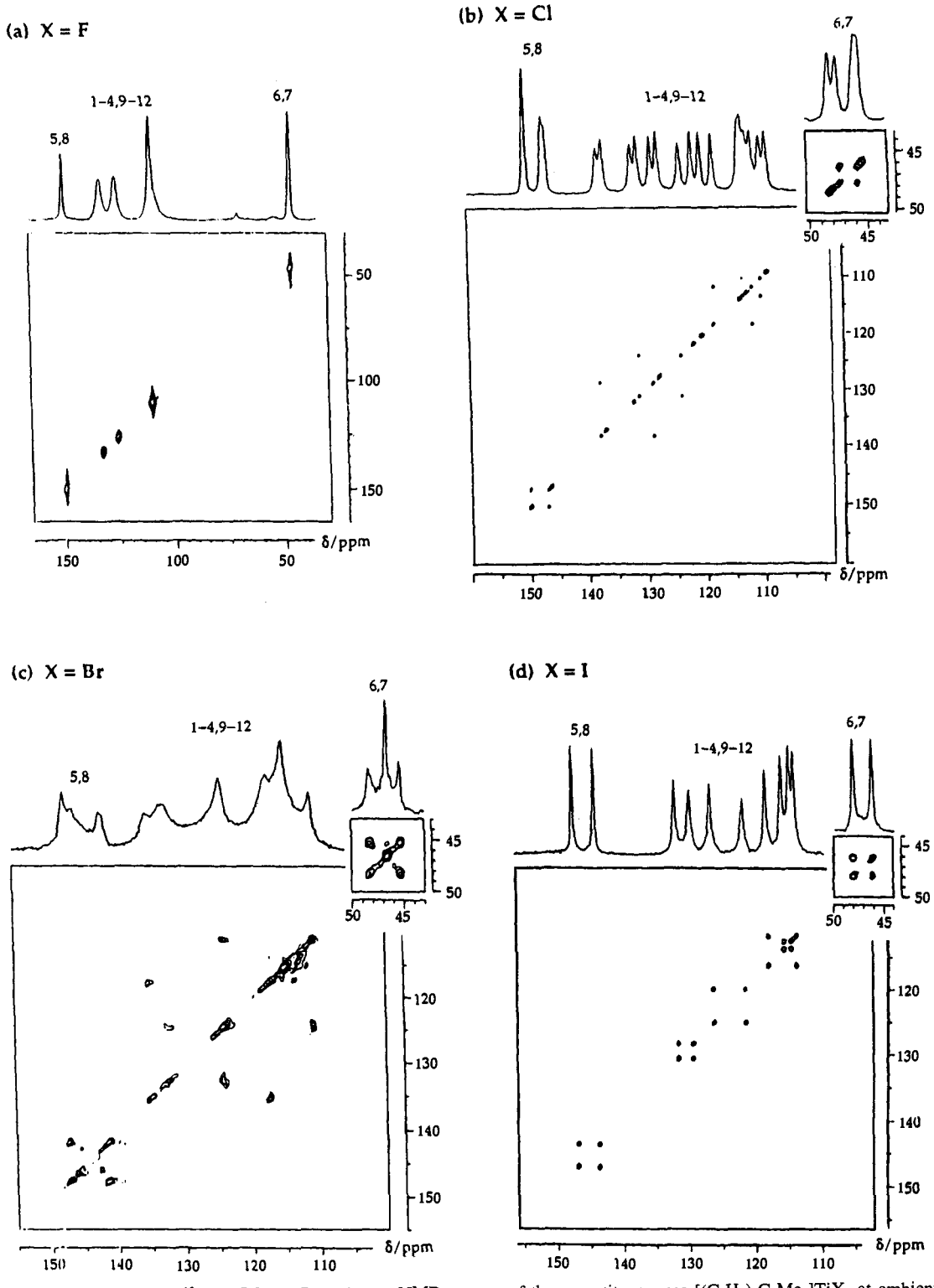

Figure 3. Phase-sensitive (TPPI) ^{13}C CP/MAS 2D exchange NMR spectra of the *ansa*-titanocenes $[(C_5H_4)_2C_2Me_4]TiX_2$ at ambient temperature and with MAS rates >4 kHz: (a) X = F (**1**), 260 t_1 increments of 60 μs with a mixing time of 1 s; (b), 512 t_1 increments of 62 μs with a mixing time of 1.5 s; (c) X = Br (**3**), 391 t_1 increments of 60 μs with a mixing time of 1 s; (d) X = I (**4**), 512 t_1 increments of 62 μs with a mixing time of 0.75 s. (Note that the methyl resonances do not appear in these spectra because they are fully relaxed within the mixing time.)

relatively sharp throughout the temperature range. The ^{13}C CP/MAS 2D exchange NMR spectrum (Figure 3b) shows that only half of the carbon resonances are undergoing a pairwise exchange with another peak in the spectrum. This suggests that one of the molecules in the asymmetric unit is undergoing an activated exchange process in a very similar manner to that found for **4**, while the other is not. Rate data were obtained, in a similar manner as for **4**, from 1D versions of the magnetization transfer experiment at temperatures in the slow limit of the exchange broadening time scale between 272 and 299 K. In these experiments, exchange was probed between the cyclopentadienyl carbon resonances at 124 and 131 ppm, shown to be connected by cross peaks in the 2D exchange experiment. Using the site permutations indicated by the 2D exchange spectrum, the high-temperature spectra line shapes were simulated for the effects of exchange broadening on one of the molecules in the structure with the assumption that the other molecule is rigid. The fit between theory and simulation, as

Table 2. Rate at Various Temperatures of the Dynamic Exchange Process Detected for the Iodide (**4**) and Chloride (**2**) Complexes

	rate of two-site exchange (k/s^{-1})	
T/K	chloride (**2**)	iodide (**4**)
265		0.2 ± 0.05^a
272	0.5 ± 0.1^a	1.5 ± 0.5^a
280	1.9 ± 0.3^a	3.6 ± 0.6^a
287	9 ± 1^a	8 ± 1^a
299	24 ± 3^a	58 ± 6^a
305		70 ± 5^b
309	70 ± 5^b	90 ± 5^b
313		140 ± 5^b
317	200 ± 10^b	210 ± 10^b
320		360 ± 10^b
324	330 ± 15^b	480 ± 10^b
328		800 ± 15^b
331	700 ± 20^b	900 ± 20^b
339	1250 ± 25^b	1500 ± 25^b
346	$1850 \pm 30^{b,c}$	$1700 \pm 30^{b,c}$
353		$1800 \pm 30^{b,c}$

[a] Data is from 1D magnetization transfer experiments. [b] Data from simulations of line shape on the basis of exchange broadening. [c] Spectra showing the onset of dipolar broadening which is not accounted for in the line shape simulation, hence values of k at these temperatures will deviate significantly from the extrapolated Arrhenius behavior.

shown for the cyclopentadienyl region of the spectrum in Figure 4b, is pleasing given the complexity of the system and demonstrates most clearly that the spectra are consistent with the mobility of one of the molecules in the structure and the rigidity of the other. The rate data are collected in Table 2 and show Arrhenius behavior for the exchange of the one molecule, $k = A \exp(-E_a/RT)$ with $E_a = 86$ kJ mol^{-1} and $A = 3 \times 10^{16}$ s^{-1}. These parameters are almost identical to those of **4**. This and the similarity of the resonance exchange pathways suggest that the dynamic processes occurring in the two cases are analogous. The ability of one molecule in the asymmetric unit to move while the other does not is of interest in respect of the manner in which intermolecular packing forces might be responsible for determining the barrier to motion.

The ^{13}C CP/MAS NMR spectrum of the bromide complex **3** at 296 K (Figure 2c) is much more complicated than those of the iodide and chloride. Some of the resonances are sharp, but most are rather broad, suggesting that chemical exchange processes leading to spectral broadening are already occurring at this temperature. The spectrum at 205 K is generally better resolved than that at 296 K, but despite the reduction in temperature, some broadening remains. The ethylene bridge carbon region of the spectrum at this temperature shows a minimum of six peaks of varying intensity, suggesting that there are at least three, probably four, molecules in the asymmetric unit of the structure. The spectra above 300 K show more dramatically the effects of exchange broadening and coalescence phenomena, such that by 340 K all the molecules in the structure appear to be involved in activated exchange processes. Thus, like the iodide homologue (**4**) and in contrast to the chloride (**2**), all the molecules in the structure appear to show dynamic behavior at increased temperature. Like the chloride (**2**), however, the crystallographically distinct molecules show different dynamic characteristics. In particular, at least one molecule is significantly more mobile than the others and its motion is not frozen out into the slow limit on the exchange broadening time scale even at 205 K. That another molecule is still in the slow limit of exchange under ambient conditions is apparent from the ^{13}C CP/MAS 2D exchange NMR spectrum at 296 K. The contour plot, shown in Figure 3c, indicates cross peaks that are consistent with a single molecule of the four undergoing slow exchange on a time scale of the order of the mixing time (1 s), very similar to that observed for **4** and **2**. The other molecules appear to be moving already at faster rates, within the exchange broadening regime. Thus in the bromide (**3**), three of the molecules are undergoing dynamics at rates in the coalescence regime by ambient temperature and the fourth, like the dynamic molecules of **2** and **4**, reaches these rates only above 300 K.

The ^{13}C CP/MAS NMR spectrum of the fluoride complex **1** at 298 K, as shown in Figure 2a, is considerably simpler than those of the other homologues. It is consistent with an asymmetric unit containing just a single molecule, and apart from the 2:1:1 peak multiplicity observed for the methyl carbons, the spectrum is indicative of 2-fold molecular symmetry. The spectrum is in fact very similar to that predicted for the iodide (**4**) at high temperatures in the fast averaging regime of its dynamic exchange process. Unlike those of the other compounds **2**–**4**, the spectrum of **1** shows little variation with temperature, the only significant change being a broadening of one of the methyl resonances at low temperature and the development of a slight splitting of the bridge carbon resonance. The broadening of a methyl group resonance of **1** at temperatures significantly below ambient is not mirrored in the spectral behavior of the other complexes. It is attributed to dipolar broadening[49] due to a slowing down of the reorientation of two methyl groups about their 3-fold axes to a rate of the order of the frequency of the high power proton-decoupling rf field (≈70 kHz). This observation is therefore a consequence of local motions of the methyl groups and is not associated with any more global molecular dynamic process. It is unusual to find methyl group reorientation slowing to these rates at such elevated temperatures, and this suggests that some of the methyl groups in the structure of **1** are rather sterically compressed. The other spectral feature of note is that the resonances of the protonated cyclopentadienyl carbons 1–4 and 9–12 remain rather broad throughout the temperature range studied. The origin of this line broadening was explored in the ^{13}C CP/MAS 2D exchange NMR spectrum at 298 K. The shape of the diagonal peaks, as illustrated in the contour plot of Figure 3a, indicates that the line broadening is homogeneous in origin[51] and therefore is not indicative of inhomogeneity of the material (in fact the sample of **1** is highly crystalline as indicated by X-ray powder diffraction). The source of the line broadening is most likely to be dipolar coupling to neighboring ^{19}F nuclei, which are closer to carbon atoms 1–4 and 9–12 than any others.

The ^{13}C CP/MAS NMR spectra of *meso*-[(1-C_5H_3-3-R)C_2Me_4(1-C_5H_3-4-R)]$TiCl_2$ (R = ^{t}Bu and 2-methylene furan) and [(1-C_5H_3-3-^{t}Bu)C_2Me_4(1-C_5H_3-4-^{t}Bu)]Ti(2,2′-biphenoxy) are all independent of temperature over the range 220–370 K and show one resonance per carbon atom in the structure. This evidence suggests that bulky substituents at any point on the molecule are liable to preclude the dynamic events.

(ii) **^{2}H NMR Spectroscopy.** It is of importance for a complete determination of the nature of the dynamic processes detected by ^{13}C CP/MAS NMR in **1**–**4** to determine the angular extent of any motions. Analysis of the spinning sideband manifolds of the MAS NMR spectra[52] allows, in principle, retrieval of the chemical shift anisotropy (CSA) of the resonances and hence information about any averaging of the CSA by motion. The CSAs of most of the carbon resonances observed here are, however, rather small and appear to change little with alterations in temperature. ^{2}H wide-line NMR through the anisotropy of its quadrupolar interaction is extremely

(51) Szeverenyi, N. M.; Sullivan, M. J.; Maciel, G. E. *J. Magn. Reson.* **1982**, *47*, 462–475.

(52) Maricq, M. M.; Waugh, J. S. *J. Chem. Phys.* **1979**, *70*, 3300–3316. Herzfeld, J.; Berger, A. E. *J. Chem. Phys.* **1980**, *73*, 6021–6030.

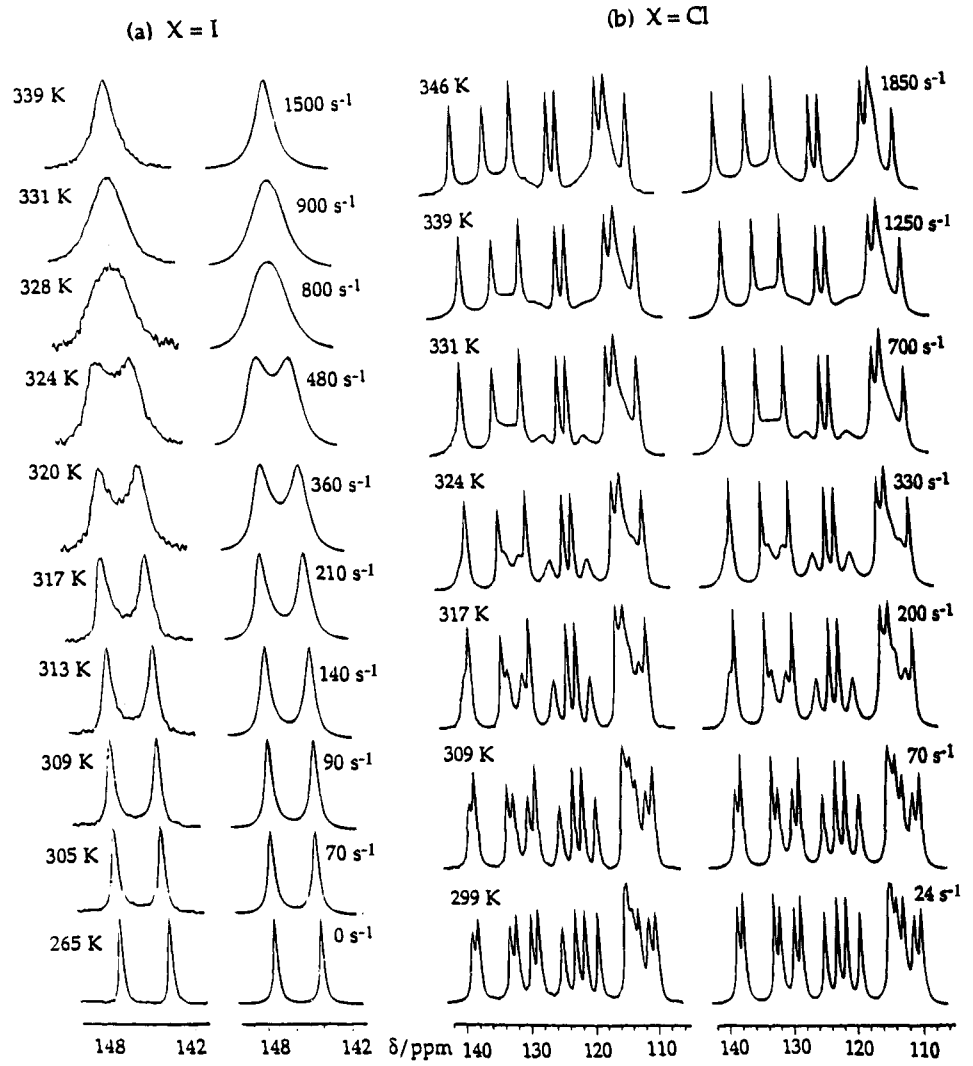

Figure 4. Comparisons of experimental ^{13}C CP/MAS NMR spectra at various temperatures and line shape simulations based on exchange broadening through a pairwise exchange process at the indicated modified two-site rate constant, k, calculated using the program DNMR4 (a) for the *ipso* cyclopentadienyl carbon resonances C_5 and C_8 of the iodide complex (**4**) and (b) for the C_1-C_4 and C_9-C_{12} regions of the chloride complex (**2**), assuming that only one of the molecules in the asymmetric structure is dynamic in the manner indicated by the 2D exchange NMR spectrum. (In each case the spectra are plotted at constant height, rather than with equal integrated area.)

sensitive to the angular extent and rate of motions over the time scale $10^{-3}-10^{-8}$ s.[37,53] ^2H NMR spectra of a powdered sample of perdeuterated **4**, taken with the quadrupolar echo sequence, are shown in Figure 5. The ambient temperature line shape shows the presence of two superimposed Pake patterns. The outer component of the spectrum is due to the C_5D_4 deuterons and the narrower superposed doublet pattern to the CD_3 deuterons whose quadrupolar interactions are averaged by reorientation of the methyl group about the $C-CD_3$ bonds. The restricted anisotropic motions expected of molecules in solids reduce the ^2H quadrupolar interaction in a manner characteristic of the spatial extent and kinetics of the motion.[37] Extrapolation of the Arrhenius relationship determined from ^{13}C CP/MAS NMR spectroscopy to 440 K suggests a rate for the dynamic process of 1.9×10^6 s^{-1}. Despite this, comparison of the patterns at 296 and 440 K shows that there is only minimal temperature dependence. This indicates either that the exchange process involves only minimal motion or that the principal direction of each deuteron electric field gradient (efg) second rank tensor changes by approximately 180° in the course of the motional event. Figure 5 shows, for comparison with the experimental spectrum at 440 K, line shapes simulated on the basis of specific motional models (*vide infra*).

(b) Single-Crystal X-ray Structure Analysis. (i) General. The structures of compounds **1**–**4** were solved from single-crystal X-ray diffraction studies. Examination of the crystal data (Table 1) shows that although these molecules are chemical homologues, the crystal structures have little obvious relationship. The structure of the fluoride (**1**) is triclinic, $P\bar{1}$, with one molecule per asymmetric unit, that of the chloride (**2**) is monoclinic, $P2_1/a$, with two molecules in the asymmetric unit, that of the bromide (**3**), is triclinic, $P\bar{1}$, with four molecules in the asymmetric unit, and that of the iodide (**4**) is rhombohedral, $R3c$, with a single molecule in the asymmetric unit. The final atomic coordinates with equivalent isotropic temperature factors are recorded in the supplementary material. Bond distances and selected interbond angles are also given in the supplementary material. The numbering follows that in Figure 1, except that for the chloride (**2**) and bromide (**3**), the leading number indicates, arbitrarily, the specific molecule in the asymmetric unit.

(ii) Molecular Dimensions. The bond lengths and interbond angles of the eight crystallographically independent molecules observed in the four crystal structures **1**–**4** are unexceptional. In each molecule the two C_5H_4 rings have a conformation that

(53) Spiess, H. W.; Silescu, H. *J. Magn. Reson.* **1981**, *42*, 381–389.

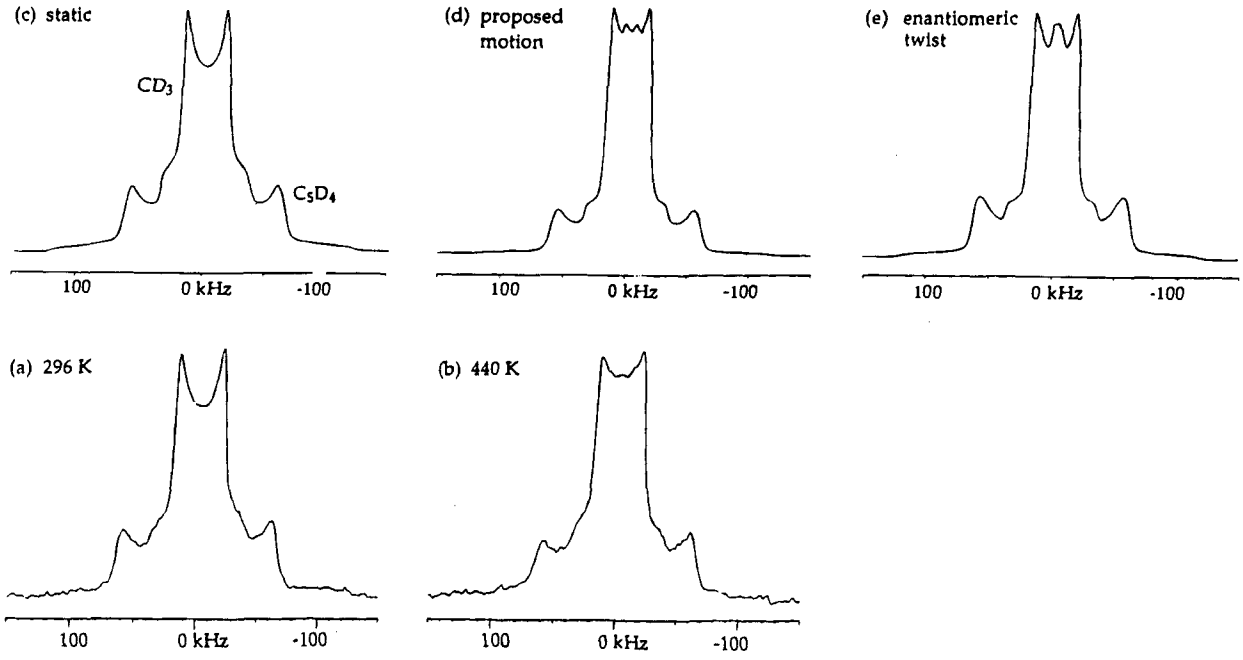

Figure 5. ^2H NMR wide-line spectra of the perdeuterated *ansa*-titanocene iodide (**4**) at (a) 296 and (b) 440 K taken using the quadrupole echo sequence with a delay of 30 μs. The wider "Pake doublet pattern" is due to C_5D_4 and the narrower to CD_3. The experimental spectra may be compared with lineshape simulations based on various dynamic scenarios: (c) no motion over and above that of the methyl groups (i.e., any motion is effectively in the slow limit on the ^2H NMR time scale, $<10^3$ s^{-1}); (d) the proposed 180° flip with polytopal rearrangement with a modified two-site rate constant of $k = 1.9 \times 10^6$ s^{-1}, as determined by extrapolation of the Arrhenius equation determined from the ^{13}C CP/MAS NMR studies; (e) enantiomeric interconversion via the ligand twist process assumed to occur in solution (see Figure 12), also at $k = 1.9 \times 10^6$ s^{-1}.

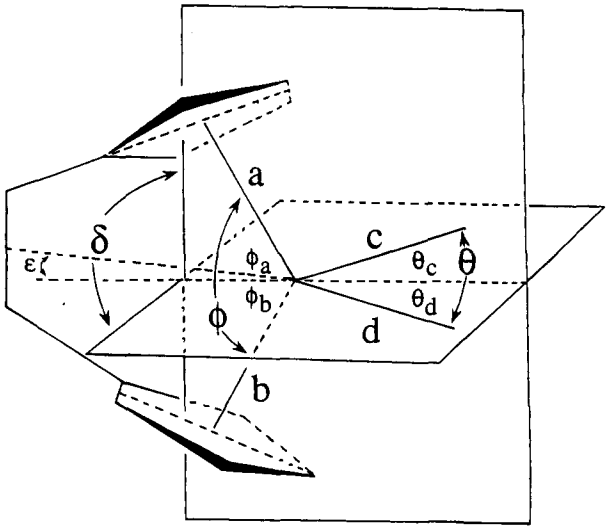

Figure 6. Schematic representation of an *ansa*-titanocene molecule detailing the dimensions listed in Table 3. *a* and *b* are the distances from the titanium atom to the centroids of the two cyclopentadienyl rings. The vertical and horizontal planes contain *a* and *b* and *c* and *d*, respectively. ϵ is the angle between the line of intersection of these planes and the line from the titanium to the midpoint of the C6–C7 ethylene bridge bond. When the molecule has a 2-fold axis, $\epsilon = 0$.

is intermediate between eclipsed and fully staggered. The molecular geometry is best described by the parameters defined in Figure 6 and listed in Table 3[54] and which indicate the remarkable similarities among the eight molecules. Two planes, one defined by the titanium atom and the centroids of the C_5H_4 rings and the other by the TiX_2 group, are always mutually perpendicular. The distance from the titanium atom to the ring centroid and the angle between the vectors from the Ti atom to each of the ring centroids vary by less than 0.025 Å and 1°, respectively, across the four complexes. Each TiX_2 plane bisects the angle between the vectors from the Ti to the ring centroids. The Ti–X bond lengths are approximately equal to the sum of the corresponding covalent radii. The X–Ti–X interbond angles in the chloride (**2**), bromide (**3**), and iodide (**4**) complexes lie in a 2° range (93.8(1)–95.9(4)°), whereas in the fluoride (**1**) an angle of 98.68(4)° is found. For each molecule the plane defined by the Ti atom and the centroids of the C_5H_4 rings bisects, approximately, the X–Ti–X interbond angles. Thus, neglecting the *ansa* bridges, the molecules have almost exact 2-fold symmetry about the line of intersection of these planes and the plane of the X–Ti–X interbond angles and have approximate C_{2v} point symmetry.

The position of the *ansa* bridge relative to the approximate molecular C_2 axis is described by the angle ϵ, the angle formed at the Ti atom between the line from the midpoint of the C–C bridgehead bond and that from the midpoint of the two halide atoms. $\epsilon = 0$ indicates 2-fold symmetry; larger values of ϵ equate to progressively larger deviations from 2-fold symmetry. The eight molecules form three groups with $\epsilon \approx 0°$, $\approx 10°$, and $\approx 20°$. Two molecules, that of the fluoride (**1**) and molecule 2 of the bromide (**3**), have $\epsilon \approx 0°$ and almost exact 2-fold symmetry, three molecules, those of the chloride (**2**) and iodide (**4**) crystal structures, deviate slightly from 2-fold symmetry ($\epsilon \approx 10°$), and the three remaining molecules, molecules 1, 3, and 4 of the bromide (**3**) crystal structure, show larger deviations from 2-fold symmetry ($\epsilon \approx 20°$).

(iii) Anisotropic Displacement Parameters. The anisotropic displacement parameters (ADPs) or thermal parameters are presented as the 50% probability ellipsoids in Figure 7. For every non-hydrogen atom in the eight independent molecules, the ADP ellipsoids are well shaped and are consistent with the representation of the molecules by TLS (torsion, libration, screw) tensors[55] of acceptable size. The largest deviations from spherical shape are found in the iodide which has the least

(54) Prout, C. K; Cameron, T. S.; Forder, R. A.; Critchley, S. R.; Denton, B.; Rees, G. V. *Acta Crystallogr.* **1974**, *B30*, 2290–2304.

(55) Shoemaker, W.; Trueblood, K. N. *Acta Crystallogr.* **1968**, *B24*, 63-76.

Table 3. Geometric Parameters As Defined in Figure 6. The Molecule is Identified by the Halogen It Contains and the Number from The Supplementary Tables

molecule	δ/deg	(a, b)/Å	ϕ/deg	(ϕ_a, ϕ_b)/deg	(c, d)/Å	θ/deg	(θ_c, θ_d)/deg	ϵ/deg
F	90.47	2.064	128.81	64.32	1.855(1)	98.68(6)	49.49	0.58
		2.064		64.49	1.854(1)		49.19	
Cl 1	90.24	2.046	127.96	64.91	2.366(1)	95.90(4)	46.9	11.18
		2.052		63.06	2.356(1)		49.0	
Cl 2	90.36	2.048	128.34	64.85	2.346(1)	94.90(4)	45.1	13.80
		2.053		63.54	2.352(1)		49.8	
Br 1	91.15	2.039	128.60	65.19	2.498(1)	94.29(5)	44.5	20.78
		2.055		63.49	2.536(1)		49.8	
Br 2	90.08	2.050	128.64	64.24	2.523(1)	96.12(5)	49.3	1.21
		2.055		64.41	2.530(1)		46.8	
Br 3	91.03	2.037	128.83	64.55	2.514(1)	94.40(5)	44.2	21.46
		2.040		64.36	2.531(2)		50.1	
Br 4	90.29	2.045	128.19	64.27	2.508(1)	94.48(5)	45.0	17.70
		2.049		63.97	2.520(1)		49.5	
I 1	90.34	2.041	128.57	64.24	2.763(4)	93.8(1)	45.7	11.73
		2.034		64.34	2.731(3)		48.1	

favorable parameter-to-observation ratio and the highest linear absorption coefficient. For all of the structures **1**–**4** the values of U_{eq}, the square of the radius of the sphere of equal volume to the ADP ellipsoid, suggest maximum root mean square atomic displacements of 0.33 Å, confirming that the ADPs are entirely consistent with thermal motion and the absence of disorder. Further, the maximum and minimum residual electron densities (Table 1) confirm that the proposed model accounts for all the electron density in each of the crystals. There is therefore no indication of any kind of disorder in any of the four crystals.

(iv) **The Crystal Structures.** The crystal structure of the fluoride complex **1** (Figure 8) consists of a single molecule in the asymmetric unit. The molecules form clearly defined layers lying parallel to the *ab* crystal plane at $c = 0.5$. Within the layers there is no evidence for affinity between the fluoride atoms, and the molecules lie with their potential 2-fold molecular axes approximately parallel to the crystallographic *b*-axis.

In the crystal structure of the chloride complex **2** (Figure 9), there are two distinct molecules of the same conformation in the asymmetric unit. These molecules are packed into sheets parallel to the *ab* crystal plane, at $z = 0$ and $z = 0.5$. Each sheet contains only one of the two crystallographically distinct molecules. The principal difference between the two layers is the relative orientation of the two molecules with respect to their neighbors. In the layer at $z = 0$ the molecules are lined up with their potential 2-fold molecular axes lying approximately parallel to the crystallographic *b*-axis, whereas in the layer at $z = 0.5$ the molecules are aligned with their potential 2-fold molecular axes at an angle of about 20° to the crystallographic *b*-axis. The overall arrangement is strikingly similar to the structure reported for the vanadium analogue of this complex,[56] and the arrangement in the layer at $z = 0$ is very similar to the arrangement found in the layers of the fluoride (**1**). In the crystal packing there is no evidence for affinity between chlorine atoms. The density of this material is slightly lower than that of the fluoride complex and deviates substantially from a clearly increasing trend in crystal density with the atomic weight of the halide.

The structure of the bromide complex **3** contains four molecules in the asymmetric unit (Figure 10). The packing observed in the crystal structure can be described in terms of layers in the [201] direction, although in this crystal each layer contains all four crystallographically distinct molecules. It is observed that seven of the eight crystallographically independent bromine atoms lie on the surface of these layers and form chains parallel to the *b*-axis.

(56) Dorer, B.; Diebold, J.; Weyand, O.; Brintzinger, H.-H. *J. Organomet. Chem.* **1992**, *437*, 245–255.

In contrast to the bromide (**3**) there is only one molecule in the asymmetric unit of the crystal structure of the iodide complex **4**, which has the same molecular conformation as observed for both molecules of the chloride complex. The complex packing arrangement in the rhombohedral cell is shown relative to the hexagonal axes in Figure 11. Perhaps the most notable feature of the crystal structure is the formation of columns parallel to the *c*-axis filled with iodine atoms. This suggests that the main structure-determining feature is the I···I interaction. This may be a consequence of the increasingly strong polarization interactions between the halogen atoms, F < Cl < Br < I. This factor could well be the explanation for the remarkable variety of structures found for four such similar, and simple, molecules.

(c) **Discussion and Conclusions.** The full structural characterization of a molecular crystal concerns not just the determination of atomic equilibrium spatial positions but also the delineation of atomic and molecular dynamics. This is recognized in X-ray diffraction by the definition of an atom in a crystal in terms of its spatial coordinates and atomic displacement parameters (ADPs, U_{ij}). In a well ordered structure the ADPs represent molecular motions that are on the infra-red time scale ($\approx 10^{-13}$ s) which is not vastly different from the time scale of interaction of X-rays with matter ($\approx 10^{-18}$ s). Slow motions are seen only if they result in positional disorder. This positional disorder is represented in the X-ray structure as either partial site occupancy or as abnormal ADPs. An X-ray structure analysis conducted at a single temperature contains little or no information about the frequency of molecular motion. CP/MAS NMR spectra provide information about the chemical nature of the molecule and the number of crystallographically distinct molecules in the asymmetric unit but they give little information about the exact conformations of the individual molecules. Additionally, and significantly, the CP/MAS NMR spectra complement and amplify the X-ray structure analysis by providing information about the slower molecular dynamic processes that occur within the NMR time scale of $\approx 10^{1}$–10^{-10} s, including the nature of the process, its frequency, and the activation barrier to motion.

For our *ansa*-titanocenes the X-ray crystal structures indicate that there are eight crystallographically distinct molecules in the four structures, one molecule in each of **1** and **4**, two in **2**, and four in **3**. These molecules may be placed in three conformational classes relating to their deviation from axial symmetry. It is of interest to compare these observations with the information that can be obtained from ^{13}C CP/MAS NMR spectroscopy. The problems encountered in a ^{13}C NMR chemical shift approach to conformational analysis of molecules

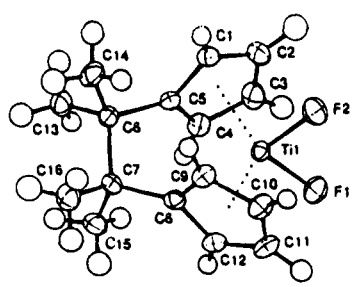

$(C_5H_4C(CH_3)_2C(CH_3)_2C_5H_4)TiF_2$

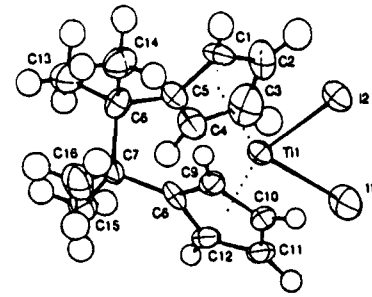

$(C_5H_4C(CH_3)_2.C(CH_3)_2C_5H_4)TiI_2$

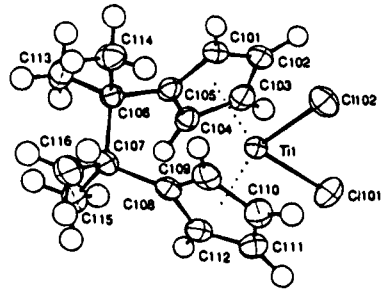

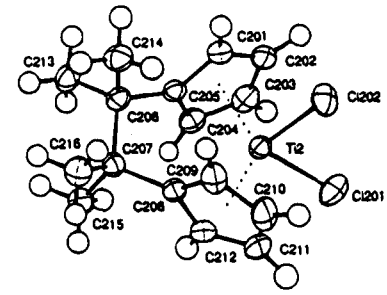

$(C_5H_4C(CH_3)_2C(CH_3)_2C_5H_4)TiCl_2$

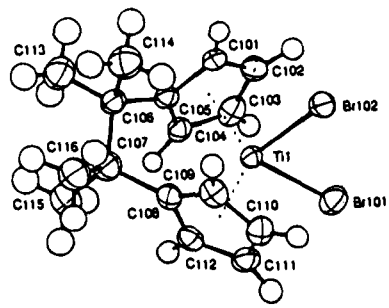

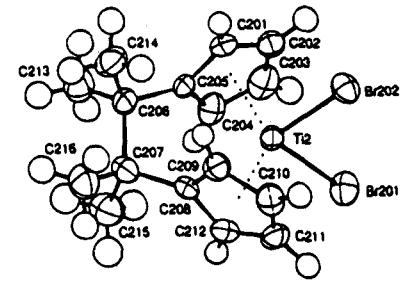

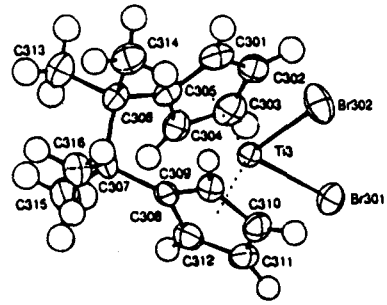

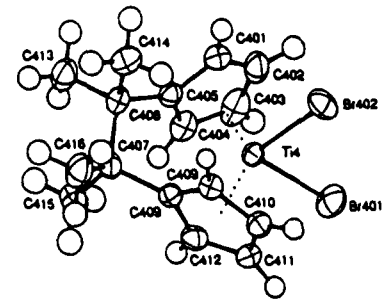

$(C_5H_4C(CH_3)_2C(CH_3)_2C_5H_4)TiBr_2$

Figure 7. Molecular conformations of the eight distinct molecules of the crystal structures of the *ansa*-titanocenes $[(C_5H_4)_2C_2Me_4]TiX_2$ (X = F, Cl, Br, I). The ADPs, shown as ellipsoids at the 50% probability level, indicate the absence of disorder or large thermal motion in any of the eight independent molecules in the four crystal structures.

in solids are illustrated in the spectrum of the chloride (**2**), in which the chemical shifts of comparable carbon atoms of the two conformationally identical but crystallographically distinct molecules are found to be substantially different (>5 ppm in some cases), presumably due to intermolecular influences. ^{13}C CP/MAS NMR spectroscopy does indicate from resonance multiplicities that for the fluoride (**1**) and iodide (**4**) there is one molecule in the asymmetric unit and for the chloride (**2**) there are two. The complexity of the NMR spectrum of the bromide (**3**) does not allow definitive identification of the multiplicity, but it is nonetheless consistent with the crystallographically determined value of 4.

The 2D exchange spectrum of the chloride (**2**) aids the NMR assignment process because it offers a "motional discrimination" of the two molecules in the asymmetric unit. Additionally, comparison of the diagonal spectrum of the 2D experiment with the conventional CP/MAS spectrum shows the improved resolution of the 2D spectrum which allows identification of distinct peaks, which appear only as shoulders in the normal spectrum, thus more accurately indicating the resonance multiplicities. The two molecules in **2** do not differ significantly in their conformations or ADPs, and without the observation of the disparate dynamic properties by NMR they would not have been seen to be especially dissimilar.

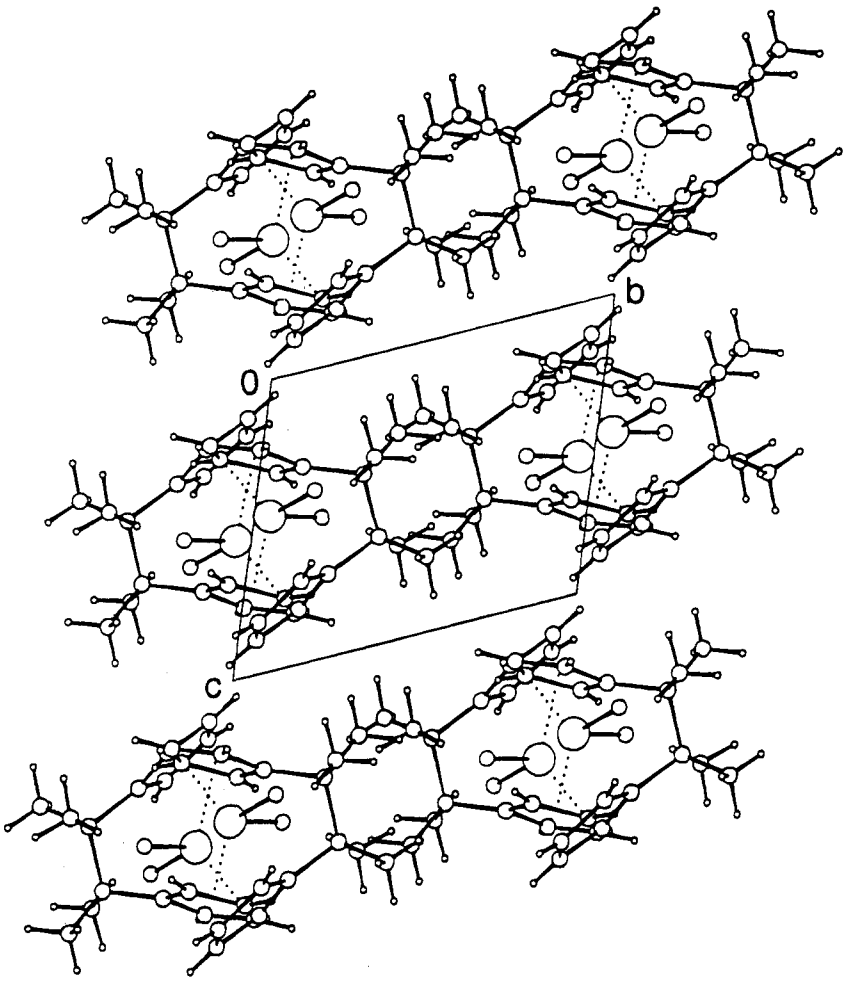

Figure 8. Crystal structure of the the *ansa*-titanocene fluoride (**1**) shown in projection down *a*, looking into the layers that are parallel to the *ab* plane.

In the 2D exchange spectrum of the bromide (**3**), the cross peaks observed demonstrate the existence of sharp resonances due to a single molecular type within the rather broad spectral envelope caused by the complex spectrum and the exchange broadening of most of the peaks of the remaining three molecules. These could not be discerned or assigned in the conventional spectrum.

^{13}C CP/MAS NMR spectroscopy indicates that in crystals **2**–**4** a pairwise activated exchange process may cause averaging in all or some of these molecules such that some crystallographically inequivalent carbon atoms become equivalent on a time average. The salient features of these dynamic processes are summarized below:

(i) The Arrhenius activation barriers to these processes have been calculated in two cases, for one molecule of the chloride (**2**), $E_a = 86$ kJ mol^{-1}, and for the iodide (**4**), $E_a = 87$ kJ mol^{-1}. These are substantial barriers, suggesting that significant atomic movement must be involved in the exchange process.

(ii) The crystal structures indicate no disorder of the molecular conformations, and therefore any rearrangement process invoked to explain the NMR spectra must not lead to a positional disordering of the atoms.

(iii) Furthermore, for the iodide (**4**) it has been shown that the averaging of the quadrupole anisotropy of the ^2H nucleus by the exchange process is minimal.

Any model proposed for the dynamic process must be consistent with all these observations, as well as accounting for the pairwise carbon nuclear exchange detected by ^{13}C CP/MAS NMR.

In order to understand the dynamic process occurring in the crystalline state, it is helpful to consider the solution NMR spectra of these compounds. ^{13}C NMR spectra in solution are simpler than even the high-temperature solid state spectra[46] and have been interpreted in terms of a rapid enantiomeric interconversion process for the individual chiral molecules. This involves a facile rearrangement of the metal polytope, illustrated in Figure 12, which cannot be frozen out even at the lowest temperatures accessible in solution. If ground-state conformations with less than C_2 symmetry, as identified in six of the eight molecules observed in the X-ray diffraction studies, persist in solution then a simple 2-fold enantiomeric interchange process is insufficient to average the NMR spectrum to the degree actually observed. It must be assumed that in solution the molecular conformational interchange is between four, not two, conformations. This overall 4-fold process still leads to an effective interconversion between enantiomers. The averaging in solution is therefore more complete than that in the crystalline state, which involves only a 2-fold interconversion.

A plausible explanation of the NMR observations of dynamic interchange in the solid state could be that molecules undergo enantiomeric conversions at crystal sites. Figure 12 shows the effect on atomic position of such a process (a) for a molecule with 2-fold symmetry, for example molecule 2 in the bromide complex (**3**), and (b) for a molecule that shows a 23° deviation from 2-fold symmetry as is the case for molecule 3 of the bromide complex (**3**). In each case the predicted mean electron density if interchange were to occur at an individual crystal site requires four "half methyl groups", two methyl groups with very

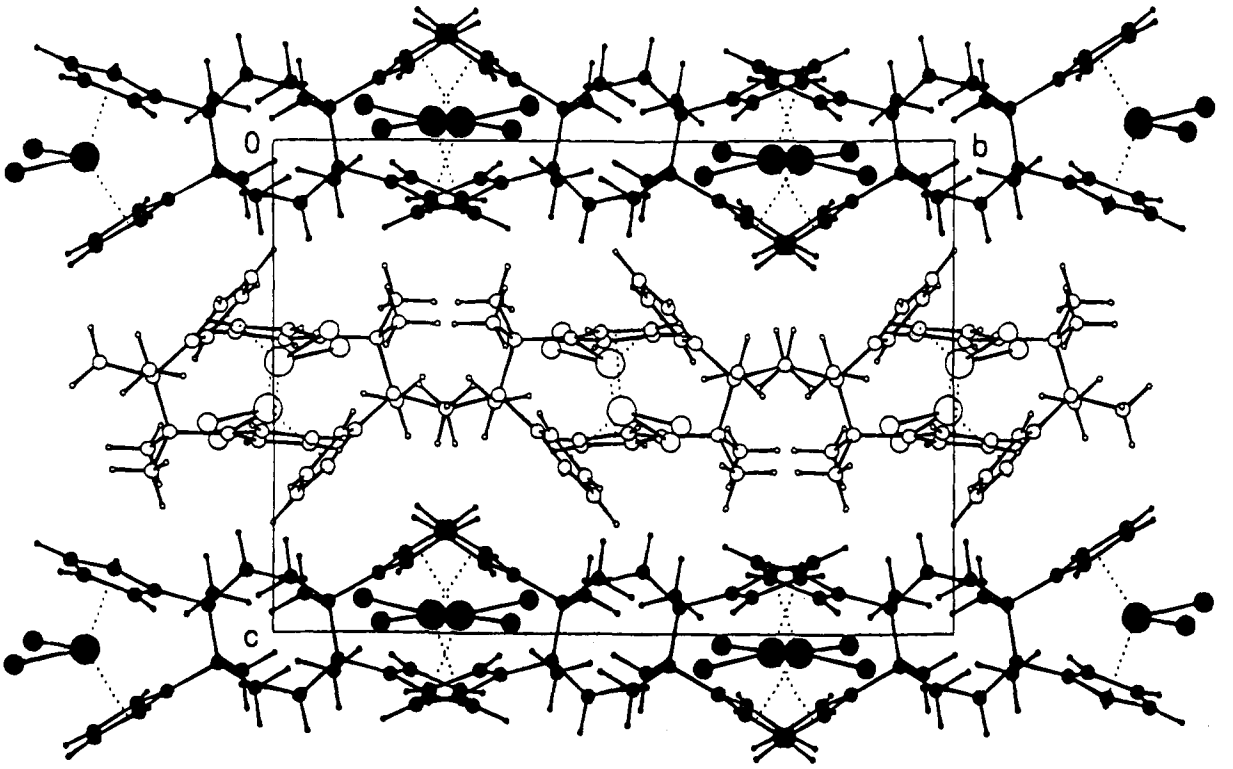

Figure 9. Crystal structure of the the *ansa*-titanocene chloride (**2**) shown in projection down *a*. The two molecules in the asymmetric unit are indicated by the filled (molecule 1) and unfilled (molecule 2) circles. The molecules are packed in two distinct layers, each layer containing only one of the two crystallographically independent molecules. The layer at $z = 0$ containing only molecule 2 shows a great similarity in packing to the layer in the fluoride (Figure 8).

large ADPs and C(6) and C(7) of the *ansa* bridge also with very large ADPs. There is no evidence for such a complex electron density for any molecule in any of the four crystal structures. Enantiomeric interconversion is thus not consistent with the X-ray data. It is equally inconsistent with the solid state ^{2}H NMR, as it would result in greater averaging of the line shape than is seen experimentally (Figure 5). Another explanation for the interconversion phenomenon must be sought.

A 2-fold reorientation of the whole molecule will interconvert the positions of those atoms seen to be exchanging in the ^{13}C CP/MAS NMR spectra. Examination of the van der Waals surfaces of (a) molecule 2 (with its almost 2-fold axis) and (c) molecule 3 (with a 23° deviation from 2-fold symmetry) of the bromide (**3**) crystal, Figure 13, shows that even for molecule 3, that with the greatest observed departure from 2-fold symmetry, the surface is approximately cylindrical. If the molecule 2 undergoes a 180° rotation about the almost 2-fold axis, the new coordinates generated very closely resemble the original, Figure 13b, and with the cylindrical shape there is little to impede such a 180° flip in the crystal. For molecule 3, with the 23° departure from 2-fold symmetry, a significant rearrangement of the metal polytope occurs through the process such that there is no net atomic positional disorder after the motional event. The lack of atomic disorder introduced by this process would be consistent with the X-ray data. Furthermore, it would not be inconsistent with the ^{2}H NMR data as a 180° flip causes no change in ^{2}H quadrupole efg tensor and the polytopal reorganization causes only small angular reorientations. A ^{2}H NMR line shape simulation calculated for a temperature of 440 K is shown in Figure 5 and matches the experimental spectrum quite well.

This process would occur if random molecular librations in the crystal allow sufficient room for an *ansa*-titanocene molecule to reorientate. When the positions of the surrounding molecules change such that the steric pressure on the dynamic molecule is reapplied, it could return to its original position or to a position involving an effective 180° rotation about the pseudo 2-fold axis. In the latter case, the positions of the halide and the cyclopentadienyl atoms are now displaced slightly from their equilibrium positions and the molecule must undergo a small polytopal readjustment. This readjustment should be a low-energy process, as judged by its easy occurrence in solution and by the existence of the different polytopal geometries in the molecules of the different crystals **1**−**4** under circumstances that appear to be dependent entirely on crystal packing forces. The expectation is that the entire process will take on the order of 10^{-14}−10^{-15} s, occurring with a relatively low frequency, e.g., for the iodide (**4**) between 10 s^{-1} at 300 K and 10^7 s^{-1} at 480 K. The net result of the process is no atomic positional disorder and since it is a rare event, as a result of the much shorter time scale of the X-ray diffraction technique, no excessively large ADPs will be observed. ^{13}C CP/MAS NMR spectra should show a pairwise averaging of the carbon resonances and the quadrupole line shape of the ^{2}H solid state NMR will be little altered. In conclusion, the evidence rules out a simple enantiomeric interchange as the explanation of the pairwise exchange process detected by ^{13}C CP/MAS NMR, but a process consisting of 180° reorientation with polytopal readjustment seems to account for the features described.

So far we have not considered whether the dynamic process occurs in the fluoride compound (**1**). Apart from the resonance multiplicities shown in the methyl and bridge carbon regions, the ^{13}C CP/MAS NMR spectrum of **1** is consistent with 2-fold symmetry down to the lowest temperature studied, 200 K, and this could potentially be interpreted as representing the fast limit of the 2-fold exchange process observed in for example the iodide (**4**). The 2:1:1 structure of the methyl peaks and the 1:1 splitting of the bridge carbon resonance (most clear at 260 K) which are inconsistent with 2-fold symmetry seem to indicate that the degeneracies of the cyclopentadienyl resonances actually

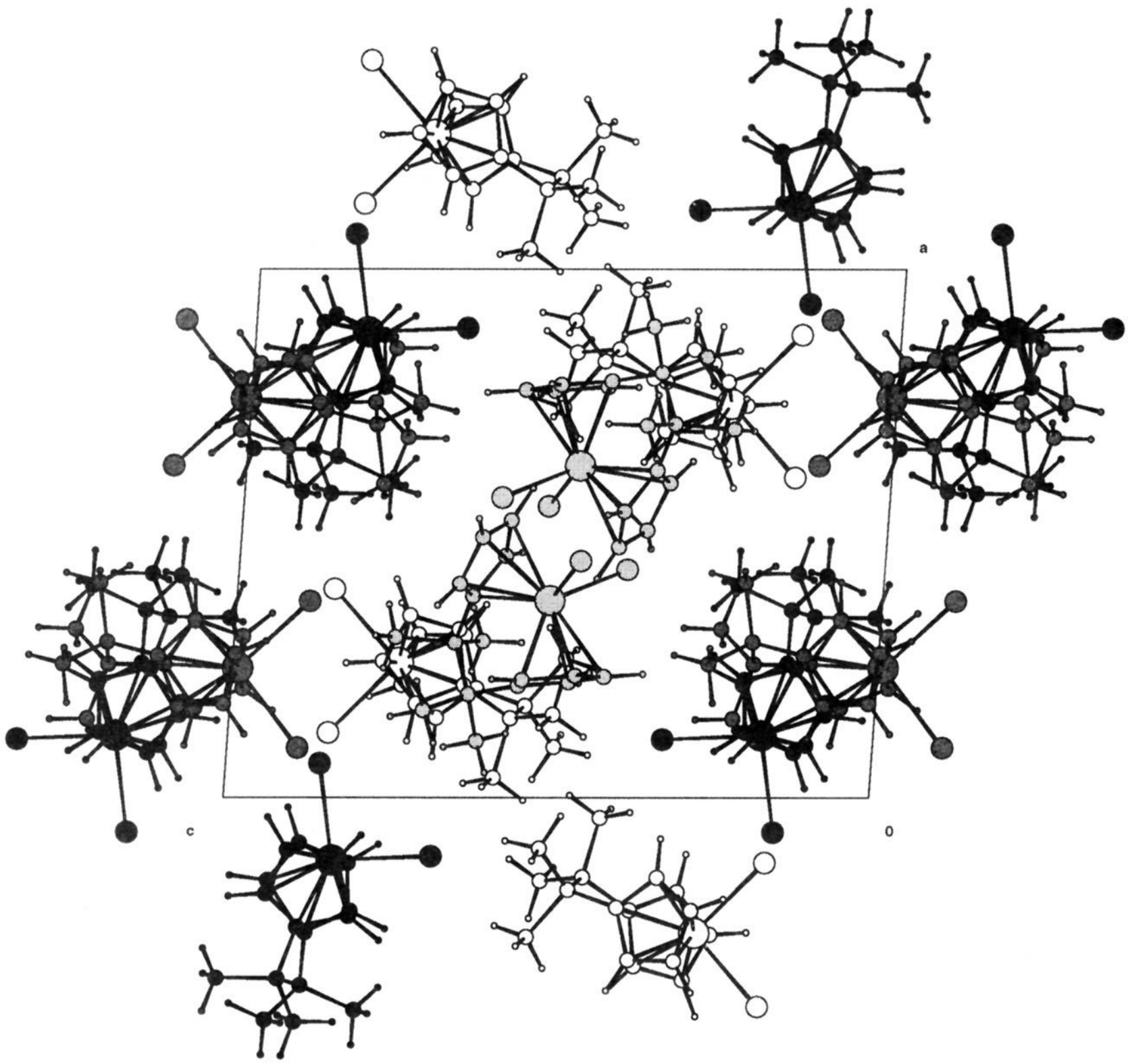

Figure 10. Crystal structure of the the *ansa*-titanocene bromide (**3**) shown in projection down *b*. The four crystallographically independent molecules of the asymmetric unit are represented by the grey scale of circles, unfilled (molecule 1), dark grey (molecule 2), black (molecule 3),and light grey (molecule 4). For molecules 1,2, and 3 the $TiBr_2$ group is in the *ac* plane and the packing shows some resemblance to that in the iodide (Figure 11), but for molecule 4 (black) the $TiBr_2$ group is approximately perpendicular to the *ac* plane.

reflect the similarity of the atomic environments caused by the noncrystallographic C_2 point symmetry of the molecules indicated by the crystal structure. The methyl groups are therefore observed to be the most sensitive probe of the true crystallographic symmetry. The axial point symmetry and the layering of the molecules in the structure of **1**, such that the pseudo-C_2 axes are parallel to those layers, might have suggested a predisposition to undergo the 180° reorientation process. In an attempt to determine whether the molecules of **1** are motional at rates that are always fast on the exchange, MAS, and dipolar-decoupling time scales of the NMR experiment, ^{13}C T_1 measurements were made; but they proved inconclusive. It does appear that the persistence of the 2:1:1 peak pattern for the methyl carbons indicates that the molecules of the fluoride complex do *not* undergo the 180° reorientation motion.

It is interesting to explore possible reasons for the dynamic behaviors of the various crystallographically distinct molecules in the structures of **2**−**4**. At any given temperature the different molecules do show different rates of motion. Some molecules of the bromide complex show exchange broadening at temperatures below ambient, while the remaining molecules of the bromide, one of the two chloride molecules, and those of the iodide show broadening and coalescence effects only above 300 K. Indeed, there is no evidence for any motion of one of the molecules of the chloride complex.

It is clear that in the chloride (**2**) and bromide (**3**) crystals, with multiple molecules in the asymmetric unit, some of the crystallographically independent molecules are more mobile than others. In particular, in the chloride (**2**) one of the two molecules undergoes pairwise exchange in the measured temperature range, but the other does not. Important in this respect is the observation that the two distinct molecular types are segregated in layers in the structure (Figure 9), each layer containing only one type of crystallographically distinct molecule. Evidently we can identify the large barrier preventing the reorientational process at one of the lattice sites with intermolecular interactions *within* the layers. If the *inter*layer interactions were unfavorable, then neither molecule type could reorient. The observation of molecular dynamics has in this manner become a very sensitive indirect probe of the intermolecular interactions. It remains to attempt to identify which of the two distinct molecules actually undergoes the dynamic process. In the layer at $c = 0$, all the

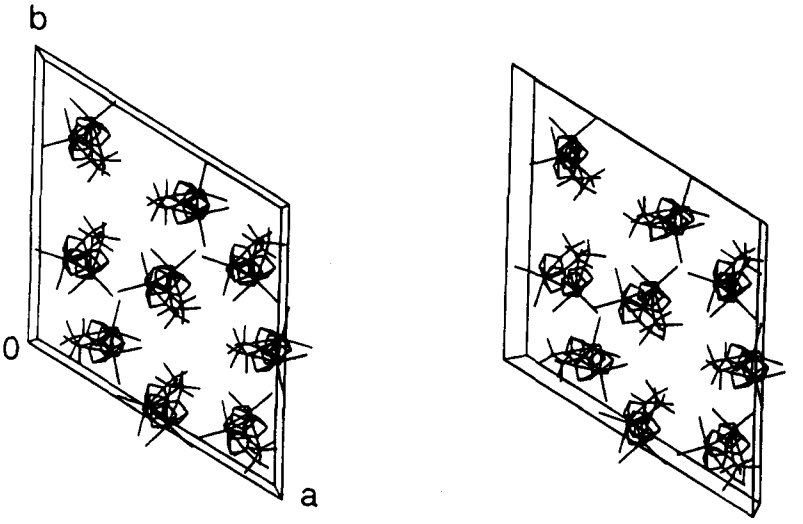

Figure 11. Eighteen symmetry-related molecules of the crystallographic unit cell of the *ansa*-titanocene iodide (**4**) shown in a stereodiagram viewed down c in the hexagonal representation of the rhombohedral cell, showing the 3-fold screw axis. For clarity the hydrogen atoms are not shown.

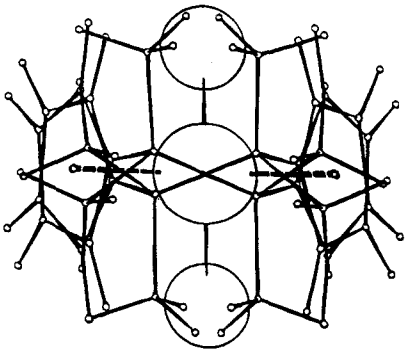

(a)

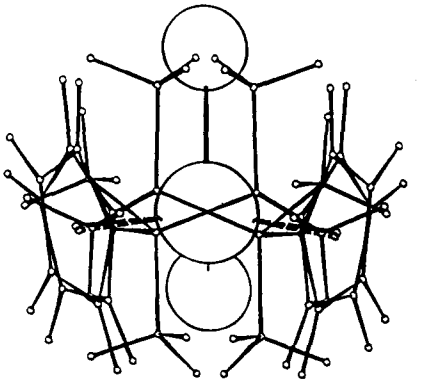

(b)

Figure 12. Superposition of enantiomers of *ansa*-titanocene conformers at a crystal site, in which the titanium atom and the center of the C6–C7 ethylene bridge bond remain undisplaced by a motion of the *ansa* ligand relative to the TiX_2 group which effectively interconverts the enantiomeric forms. The diagram shows the effect on atomic positions expected to be observed in an X-ray crystal structure analysis if the molecule underwent an enantiomeric conversion at a crystal site with least possible atomic rearrangement, (a) for a molecule with 2-fold symmetry and (b) for a molecule that shows a deviation from 2-fold symmetry of $\epsilon = 23°$.

molecules lie with their near-cylindrical axes approximately parallel and coplanar like a set of neatly aligned barrels on a flat surface. In fact there is a striking similarity between this layer and the single layer observed in the fluoride (**1**) structure. In the layer at $c = 0.5$, by contrast, the cylindrical axes are neither parallel to nor coplanar with the layer, and crude approximations suggest that this layer occupies a greater volume (i.e., has a lower density) than that at $c = 0$. Thus it can be hypothesized either that cooperative motions might make it easier for the aligned cylinders in the layer at $c = 0$ (molecule 2) to reorient than the ill-aligned molecules (molecule 1) in the layer at $c = 0.5$ or that the lower density of the layer at $c = 0.5$ allows molecules more space to reorient. The identity of the dynamic molecule in the structure of **2** remains impossible to determine.

Identification of particular dynamic behavior with specific molecules of the bromide (**3**) structure also proves impossible, especially since the layers occurring in this structure contain all of the distinct molecular types, and an intermolecular packing analysis in the manner of the chloride is not possible. In the ^{13}C CP/MAS NMR spectrum of the bromide (**3**) at 205 K, the observation of resonances that are still exchange broadened indicates that at least one of the molecules in the asymmetric unit is undergoing the exchange process at a rate that is still significant on the NMR exchange broadening time scale. The 2D exchange spectrum at 296 K demonstrates that one molecule is dynamic but at a rate still in the slow limit of the exchange broadening regime under ambient conditions, rather like the iodide and the dynamic molecule of the chloride. Finally, the spectrum at 340 K shows conclusively that all the molecules in the structure are dynamic by this temperature. It is possible to focus on the different classes of molecular conformation constituted by the individual molecules of the bromide structure. The X-ray analysis shows that one molecule, molecule 2, has almost exact 2-fold symmetry. Once reoriented by 180°, no relaxation of the molecular conformation is necessary to fit the crystal site. Thus, it might be imagined intuitively that the energy barrier to rotation for molecule 2 could be less than that for the other three and that the pairwise exchange is faster. However, molecules of the fluoride complex **1** have similar axial symmetry, yet they are not dynamic. In addition, the ^{13}C CP/MAS NMR spectrum of the fluoride suggests that for any axially symmetric molecule the chemical shifts of the resonances which would undergo mutual exchange are likely to be similar or even degenerate, and consequently any exchange broadening effects would be expected to be rather small. Clearly it is not possible

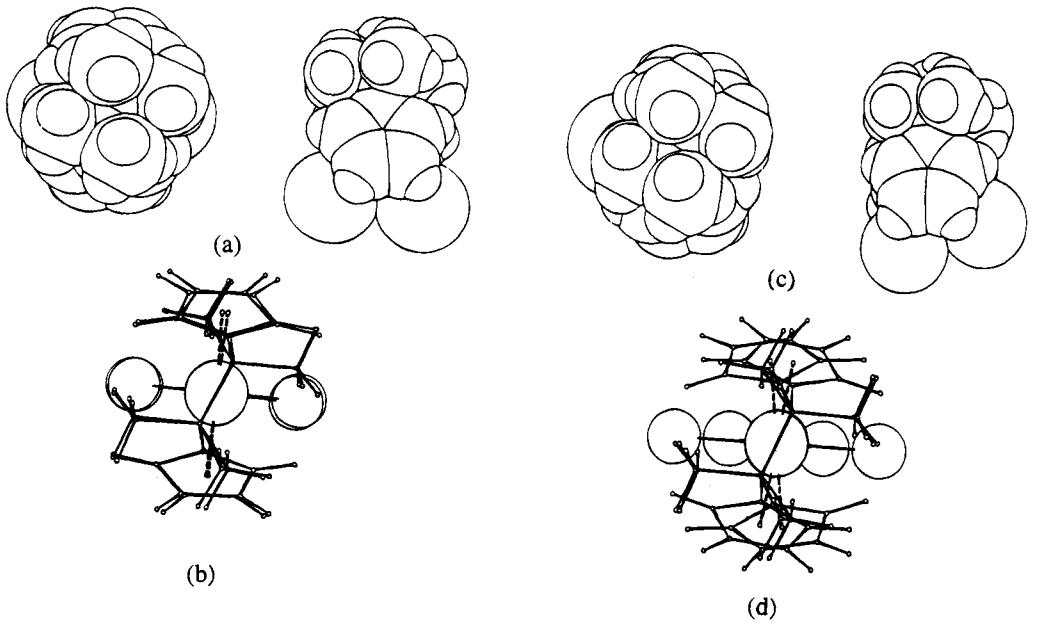

Figure 13. van der Waals surfaces of (a) molecule 2 of the bromide with near 2-fold symmetry and (c) molecule 3 of the bromide crystal with the greatest departure from 2-fold symmetry ($\epsilon = 23°$) of the eight molecules observed, showing that in each case the molecules are approximately cylindrical. In (b) and (d) the molecules are shown superimposed in each case on their 2-fold rotamer about an axis through the midpoint of the C6–C7 ethylene bridge bond and the titanium atom.

to link molecule 2 of the bromide structure to the molecule(s) identified by NMR as undergoing the most facile dynamics. Equally, the 2D exchange spectrum indicates a molecule which is uniquely dynamic on the time scale (ca. 1 s) of this experiment, and the pattern of the resonances observed suggests that they belong to a molecule of nonaxial conformation. The three nonaxial molecules all have very similar conformations ($\epsilon \approx 20°$), and it is not possible from a study of the crystal structure to identify an especially unique lattice site with this particular dynamic behavior.

The analysis of the bromide (**3**) crystals, in which three of the molecules show the greatest deviation from axiality discovered throughout the four structures, yet in which all the molecules show the activated exchange process in the NMR spectra, reinforces the viewpoint that all of the molecules are fairly cylindrical, whatever their degree of deviation from axiality, and are therefore potentially dynamic. The observed dynamics of any particular molecule probably reflect the intermolecular interactional profile, and any conformational readjustment of the ligand polytope required to preserve atomic order at crystal lattice sites is clearly extremely facile in comparison with the barrier to the 180° jump part of the overall composite process invoked.

It is particularly striking that there is a wide variation in the structures adopted by these materials, yet where comprehensive rate data have been obtained, in the case of the iodide (**4**) and chloride (**2**), the Arrhenius parameters show remarkable similarities. The reason for the three distinct classes of deviation from molecular axiality in these structures remains obscure, but certainly their observation in this homologous series of compounds supports Burger *et al.*'s[5] conclusion from molecular mechanical calculations that only weak interactions are necessary to cause changes in the conformations of the *ansa* ligands in these metallocenes. We would also like to draw attention to the variation with halogen identity of the number of crystallographically distinct molecules in each structure. In the case of the fluoride (**1**), the dominant intermolecular contacts are those between atoms of the *ansa* ligand, the van der Waals volume of the fluorine atoms being rather small such that they are largely hidden from intermolecular interactions. The helical chain of iodine atoms observed in the structure of **4** indicates that maximization of interactions between the large, polarizable iodine atoms may be the driving force for its adoption. For the chloride (**2**) and bromide (**3**) the forces involving the maximization of halogen–halogen interactions and the ordering of contacts involving hydrogen atoms may be of similar magnitude, and this might lead to the structural diversity of these particular crystals and the 2- and 4-fold multiplicities observed in their asymmetric units. Further work will be necessary to determine whether this is significant or merely a coincidence.

It is significant that the mechanism for the motion detected in these crystals which is most consistent with all the observed experimental data is essentially an overall molecular reorientation with concomitant conformational readjustment. This is in contrast to most other cases of motions in molecular crystals such as our previously reported work on potassium penicillin V[57] or titanium tetracyclopentadienyl,[58] in which only individual segments of the molecules are engaged in dynamic processes. The motion observed in the solid state contrasts strongly with the extensive and facile conformational flexibility of the *ansa*-titanocenes in solution. This demonstrates that the forces controlling the packing of these molecular crystals, while able to tolerate a motional event of large angular extent, are able to force the molecules to adopt conformations well-ordered by lattice site. Such angularly specific overall molecular motions are well established in host–guest chemistry,[59] and there is an example of rotoreptation in adducts of 18-crown-6,[60] but they are less familiar in pure molecular crystals, where reports to date concentrate on simple cyclic systems.[61,62] Additionally, it

(57) Fattah, J.; Twyman, J. M.; Heyes, S. J.; Watkin, D. J.; Edwards, A. J.; Prout, K.; Dobson, C. M. *J. Am. Chem. Soc.* **1993**, *115*, 5636–5650.
(58) Heyes, S. J.; Dobson, C. M. *J. Am. Chem. Soc.* **1991**, *113*, 463–469.
(59) Ripmeester, J. A.; Ratcliffe, C. I. In *Inclusion Compounds*; Atwood, J. L., Davies, J. E. D., McNicol, D. D., Eds.; Oxford University Press: Oxford; 1991; Vol. 5, pp 37–89. Clayden, N. J.; Dobson, C. M.; Heyes, S. J.; Wiseman, P. J. *J. Inclusion Phenom.* **1987**, *5*, 65–68.
(60) Ratcliffe, C. I.; Ripmeester, J. A.; Buchanan, G. W.; Denike, J. K. *J. Am. Chem. Soc.* **1992**, *114*, 3294–3299.
(61) Mack, J. W.; Torchia, D. A. *J. Phys. Chem.* **1991**, *95*, 4207–4213
(62) Parsonage, N. G.; Staveley, L. A. K. *Disorder in Crystals*; Clarendon Press: Oxford, 1978.

is important to realize that the reorientational motion in the *ansa*-titanocenes is not as extreme as that typical of plastic crystal phases, in which the molecules typically undergo dynamics leading to atomic disorder and phases of cubic symmetry.[62,63] Also, since the motional process detected in the *ansa*-titanocenes produces no atomic disorder, there is no configurational entropy inherent in the process, and these materials do not show any sign of a phase transition before melting. Instead, the present reorientational motions appear to occur within the constraints of low-symmetry crystal structures with large activation barriers.

In conclusion, the ^{13}C CP/MAS NMR spectra of this homologous series of *ansa*-metallocenes provide clear evidence for occurrence of an activated dynamic process, which is effectively invisible to the X-ray diffraction experiment. Two hypotheses as to the nature of the motion have been tested here. One, involving simple enantiomer interchange on individual sites in the crystal, can be eliminated by examination of the X-ray data and ^{2}H NMR spectroscopy. We propose instead a motional process involving 2-fold reorientation with a small polytopal readjustment, which is consistent with all the present experimental results. This study is a further example of the powerful synergism between the experimental techniques of solid state NMR and X-ray diffraction.[57] It provides further evidence that in crystals substantial molecular motion may take place in the absence of any major disruptions to the crystal lattice.

(63) Sherwood, J. N. Ed. *The Plastically Crystalline State*; Wiley: Chichester, 1979. Johnson, R. D.; Bethune, D. S.; Yannoni, C. S. *Acc. Chem. Res.* **1992**, *25*, 169−175.

Acknowledgment. We thank Prof. H.-H. Brintzinger for originally stimulating this work and for useful comments and suggestions and Prof. G. Engelhardt, Dr. P. Burger, and Dr. J. Diebold for helpful discussions. We thank the SERC and the Royal Society European Exchange program (S.J.H.) for funding.

Supplementary Material Available: Tables of atomic coordinates, atomic displacement parameters, and bond distances and angles (35 pages). This material is contained in many libraries on microfiche, immediately follows this article in the microfilm version of the jounal, can be ordered from the ACS, and can be downloaded from the Internet; see any current masthead page for ordering information and Internet access instructions.

JA943253Z